Assignment of the vibrations of the S_0, S_1 and D_0^+ states of perhydrogenated and perdeuterated isotopologues of chlorobenzene

Anna Andrejeva, William D. Tuttle, Joe P. Harris and Timothy G. Wright[a]

School of Chemistry, University of Nottingham, University Park,

Nottingham NG7 2RD, UK

[a] Corresponding author. Email: Tim.Wright@nottingham.ac.uk

Abstract

We report vibrationally-resolved spectra of the $S_1 \leftarrow S_0$ transition of chlorobenzene using resonance-enhanced multiphoton ionization (REMPI) spectroscopy. We study chlorobenzene-h_5 as well as its perdeuterated isotopologue, chlorobenzene-d_5. Changes in the form of the vibrational modes between the isotopologues and also between the S_0 and S_1 electronic states are discussed for each species. Vibrational bands are assigned utilizing quantum chemical calculations, previous experimental results and isotopic shifts, including those between the ^{35}Cl and ^{37}Cl isotopologues. Previous work and assignments of the S_1 spectra are discussed. Additionally, the vibrations in the ground state cation, D_0^+, are considered, since these have also been used by previous workers in assigning the excited neutral state spectra.

I. INTRODUCTION

Monosubstituted benzene molecules are of great interest spectroscopically, as they are the simplest deviation from the parent benzene molecule; but also a number of them provide links to the building blocks of biological molecules. The simplest types of monosubstituted benzenes are the monohalobenzenes. In the following, we shall abbreviate the titular molecule, chlorobenzene, as ClBz; in addition, we shall indicate the isotopologue with a presuperscript, 35 or 37, and/or a suffix -h_5 or -d_5 as appropriate, so that ^{37}ClBz-d_5 represents the ^{37}Cl isotopologue of the perdeuterated chlorobenzene molecule, for example. We shall also frequently refer to fluorobenzene, which will be denoted FBz.

It is well known that intense, non-totally-symmetric fundamentals are seen in electronic spectra of the $S_1 \leftarrow S_0$ transition for substituted benzenes. (These modes are specifically of b_2 symmetry for monosubstituted benzenes, where we are locating the planar molecule in the *yz* plane.) The appearance of these bands arises from Herzberg-Teller vibronic coupling between

the S_1 ($\tilde{A}\,^1B_2$) state and a higher-energy $^1A_1$ state;[1] the coupling occurs via various b_2 vibrations, and so these appear in the spectrum.

A. Neutral ClBz-h_5

There has been a significant number of studies performed on the ClBz-h_5 molecule, making it one of the most-studied monosubstituted benzenes. Ground state vibrational wavenumbers of ClBz-h_5 have been obtained from infrared (IR) and Raman studies and summarized by Whiffen.[2] Early studies of the $S_1 \leftarrow S_0$ transition were reported by Purvis,[3] while Sponer and Wollman[4] recorded the first vibrationally-resolved UV absorption spectra of ClBz-h_5 at different temperatures in 1941. Subsequently, a higher-resolution study by Cvitaš and Hollas[5] was reported in 1970, where the spectra were partially rotationally-resolved, with the measured origin position at 37048.2 ± 0.2 cm^{-1}. Perhaps the most comprehensive study of this transition was undertaken by Jain, Bist and coworkers[6,7,8] who assigned the majority of the normal modes in the ground and first electronically-excited states, reporting them in a series of publications divided into: planar vibrations of the S_1 state;[6] planar vibrations of the S_0 state;[7] and out-of-plane vibrations of the ground and excited states.[8] The assignment of the vibrations in the S_0 state has been discussed by our group in ref. 9.

Over the last 30 years, a number of groups have conducted resonance-enhanced multiphoton ionization (REMPI) spectroscopic studies on the ClBz-h_5 molecule under cold jet conditions and have provided assignments of the vibrational structure in the S_1 state.[10,11,12] It is noted that the experiments of Murakami et al.[10] are two-photon excitation, followed by ionization, while the experiments by Anderson et al.[11] and Walter et al.[12] are one-photon excitation followed by ionization. The Ortiz group[13] have also employed high-resolution, one-photon excitation REMPI spectroscopy in a supersonic beam, to obtain photoionization spectra of the origin band of the S_1 state of the ^{35}ClBz-h_5 and ^{37}ClBz-h_5 molecules at a rotational temperature of 1 K; this allowed them to determine the shift of the origin band between the $^{35/37}$Cl isotopologues. They report a shift of 0.14 ± 0.02 cm^{-1}, which is within the resolution of the present work, and hence we do not expect to be able to discern this; however, shifts of vibrational bands can be larger, and this will be commented on later. To our knowledge, Imhof and Kleinermanns are the only group to date to have reported a laser-induced fluorescence spectrum of ClBz, also dispersing the fluorescence from several S_1 vibrational states.[14] Other workers have reported a lack of success in obtaining fluorescence spectra of

ClBz using discharge lamps[15] or electron impact,[16,17,18] even though resolved spectra for benzene and FBz were so-obtained.

B. Neutral ClBz-d_5

ClBz-d_5 is much less studied compared to its non-deuterated isotopologue. The vibrational spectrum, using IR and Raman spectroscopies, has been reported by Nanney et al.[19] Assignments were made both in terms of symmetry and an approximate description of the atomic motions; comparison was also made to the wavenumbers of the corresponding vibrations in ClBz-h_5, FBz-h_5 and isotopologues of benzene. These vibrations were labelled by Varsányi in his book[20] (see below and Table 1). The recording of the $S_1 \leftarrow S_0$ REMPI spectrum is implied in a paper by Asselin et al.;[21] however, no spectra are reported therein, as the emphasis was on REMPI photoelectron spectra (REMPI-PES).

C. Cations

A number of photoelectron studies have gained information on the vibrations in the ClBz-h_5^+ cation, covering conventional HeI PES,[22] REMPI-PES,[11,12,21] multiphoton dissociation spectroscopy[23], zero-electron-kinetic energy (ZEKE) spectroscopy, [24] and also one-photon[25] and two-photon, two-colour[26] mass-analyzed threshold ionization (MATI) spectroscopy. These are vibrationally-resolved to varying extents and we shall discuss the assignments in these papers below. This is pertinent to the assignment of the S_1 vibrations, since in the two-colour experiments, the assignment of the cation vibrations has often been used to infer the nature of the intermediate vibrational level (or vice versa). We also note that Asselin et al.[21] recorded REMPI-PES spectra of ClBz-d_5.

D. Vibrational nomenclature

In previous work, the majority of the assignments of the vibrational bands have been in terms of Wilson[27] or Varsányi notation.[20] The Wilson labels are based upon the vibrations of the benzene molecule, whose form changes considerably upon substitution. This issue has been highlighted for the FBz molecule by Butler et al.,[28] Pugliesi et al.[29] and ourselves,[9, 30] where it has been shown that the Wilson labels are inappropriate for describing the phenyl ring-localized vibrations in substituted benzenes. In Table 1 we show how the vibrations of ClBz can be expressed in terms of the Wilson benzene modes, where it can be seen that many modes are very mixed versions of these. (These mixings, obtained at the B3LYP/aug-cc-pVTZ level, are very similar to those in ref. 9.)

The alternative Varsányi notation[20] is also of limited use because of its arbitrary division of the substituents into heavy or light groups, which leads to the same vibrational mode being represented by different labels in even quite similar molecules. This aspect is particularly relevant here, as F was considered a "light" substituent and Cl was considered a "heavy" substituent; thus, a number of vibrations are given different labels in FBz and ClBz, despite the fact that, as we showed in ref. 9, the atomic motions of the vibrations in the two molecules are very similar. An additional point of confusion is that the Varsányi notation uses the Wilson-type labels for often very different vibrational motion.

The alternative Mulliken[31] notation (sometimes referred to as Herzberg notation[32]) is based upon the numbering of the vibrations in order of decreasing wavenumber in symmetry blocks. These are specific to each molecular point group and are in a predetermined order and so the numbering will change for different molecules. Problems arise even for monatomic substituents, where the mass effect may be enough to change the ordering of the vibrations, leading to different Mulliken labels being given to ostensibly the same vibration. To circumvent these issues, we have put forward a consistent method for labelling the ring-localized vibrational modes of monosubstituted benzenes,[9] where the same vibrational modes have the same unique label, M_i, irrespective of a substituent that is present in the molecule, as seen in our work on toluene.[33,34] This labelling will be used in the present work for the S_0 state. (The motion of the atoms in each mode is presented in Figure 5 of ref. 9.)

We shall examine the changes in the vibrational modes upon electronic excitation (a Duschinksy rotation[35]), and will also examine the vibrations in perdeuterated ClBz via a generalized Duschinksy rotation.

E. Present work

We employ one-colour REMPI spectroscopy to record rotationally-cold, vibrationally-resolved electronic spectra of the $S_1 \leftarrow S_0$ transition in ClBz-h_5 and ClBz-d_5, for each of their ^{35}Cl and ^{37}Cl isotopologues. The spectra are assigned using the observed experimental isotopic shifts, employing available previous experimental and theoretical results, and additionally quantum chemical calculations for all of the isotopologues, carried out in the present work. The REMPI spectrum of ClBz-d_5 is reported here for the first time and, as with our previous work on FBz,[30] we examine how the vibrations in the perdeuterated isotopologue compare to those of the perhydrogenated molecule. In addition, we highlight the

mixing of the vibrational modes that occurs between the S_0 and S_1 states for each isotopologue. In some cases, comparison between the activity seen in ClBz with that seen in FBz and toluene is insightful.

We shall also examine the vibrations of the ground state cation and assign these with M_i^+ labels, to be consistent with the S_0 and S_1 vibrations; particularly the latter are frequently assigned via activity seen in two-colour photoionization techniques, as mentioned above. We shall also discuss the dispersed fluorescence (DF) spectra of ref. 14 in the light of the above discussion, where some anomalies will be highlighted.

II. EXPERIMENT

The third harmonic (355nm) of a neodymium-doped yttrium aluminium garnet laser (Nd:YAG, Surelite III, 10Hz) was used to pump a tuneable dye laser (Sirah Cobra Stretch), operating on Coumarin 503. The fundamental output of the dye laser was frequency doubled by a BBO crystal in order to obtain tuneable UV radiation across the wavenumber region of interest.

ClBz-h_5 (Aldrich, 99.8% purity) or ClBz-d_5 (Aldrich, 99 atom% D) vapour, each with the naturally-occurring ratio of ^{35}Cl:^{37}Cl, was seeded in ~5 bar of argon carrier gas and the gaseous mixture was passed through a General Valve pulsed nozzle (750 μm, 10 Hz, opening time of 150 μs) to create a free jet expansion, and hence almost all transitions are from the ground state zero-point vibrational level. The focused, frequency-doubled output of the dye laser passed through a vacuum chamber where it perpendicularly intersected the free jet expansion between two biased electrical grids located in the extraction region of a time-of-flight spectrometer. After (1+1) ionization occurred, the resulting ions were extracted and detected by a dual microchannel plate (MCP) detector. The signal was passed to an oscilloscope (LeCroy LT342 Waverunner) for monitoring, and a boxcar (SRS SR250) for integration and averaging; the averaged signal was then relayed to a computer for storage and analysis. The timing of the laser pulse relative to the opening time of the pulsed nozzle was controlled using a digital delay generator. The delays were varied to produce optimum conditions to ensure that the coldest part of the beam was probed.

III. COMPUTATIONAL METHODOLOGY

In order to aid in the assignment of the spectra, the vibrational frequencies of each molecule were calculated using the GAUSSIAN 09 software package.[36] For the S_0 ($\tilde{X}\ ^1A_1$) state and the

ground cation ($\tilde{X}\,^2B_1$) state, (U)B3LYP/aug-cc-pVTZ calculations were used; whereas for the S_1 ($\tilde{A}\,^1B_2$) state TD-B3LYP/aug-cc-pVTZ calculations were employed. All of the harmonic vibrational frequencies were scaled by the usual factor of 0.97. For the unrestricted calculations $<S^2>$ values were all ~ 0.76 showing that spin contamination was minimal.

The vibrational modes of the S_0 state were labelled by comparing the molecular vibrational displacements with those of FBz via a generalized Duschinsky matrix approach employing the FC-LabII program,[37] as discussed in ref. 9. This provided a clear assignment of the phenyl ring-localized vibrations. For ClBz-d_5, the molecular vibrational motions were compared to those of ClBz-h_5 in the S_0 state via a generalized Duschinsky approach using FC-LabII. Similarly, vibrations in the S_1 and D_0^+ states are compared to those of the respective S_0 state, and those of the respective S_1 and D_0^+ states were compared with each other.

IV. RESULTS AND ASSIGNMENTS

A. Overview of the $S_1 \leftarrow S_0$ spectra.

The (1+1) REMPI spectra of ClBz-h_5 (upright, top trace) and ClBz-d_5 (inverted, bottom trace) from 0 – 3000 cm^{-1} are shown in Figure 1; only the spectra for the ^{35}Cl isotopologues are shown. We shall comment on the spectra of the ^{37}ClBz isotopologues as required, but suffice to say at this point that they are very similar, with generally only small isotopic shifts.

We estimate our relative band positions to be precise to ± 0.5 cm^{-1}. By simulating the band origin using PGOPHER[38] using the rotational constants reported in ref. 5, it was possible to compare to the band profile presented in the latter work, and so calibrate the ^{35}ClBz-h_5 spectrum to their band origin of 37048.2 ± 0.2 cm^{-1}; this showed that the rotational temperature in the present work was around 5 K. It was then found that the position of the ^{37}ClBz-h_5 origin band was at the same position, within our experimental uncertainty, showing that the S_1 origin bands of the ^{35}Cl and the ^{37}Cl isotopologues are within 0.2 cm^{-1} of each other, in agreement with the result of de la Cruz et al.[13] For the ClBz-d_5 origin transition, an isotopic blue shift of 167.4 cm^{-1} is determined from our spectra, which puts the origin at 37215.6 ± 0.5 cm^{-1}; this is in reasonable agreement with the band position of 37218.1 cm^{-1} reported by Dimicoli and coworkers.[21]

The spectra presented in Figure 1 have been plotted on a relative scale, with the origin transitions each shifted to zero for straightforward comparison between the different isotopologues. (Since we are working under jet-cooled conditions, almost all observed

transitions are from the ground state zero-point vibrational level, and so we indicate the assignment of each vibronic transition with only the upper state vibrational level; note that M_x^n implies a transition to a vibration with n quanta of the M_x vibration, from the ground state zero-point vibrational level.) Our vibrational bands are not fully rotationally resolved in either the ClBz-h_5 or ClBz-d_5 spectra, and so we have employed the wavenumber of the most intense part of each vibrational band, in order to calculate consistent vibrational spacings. The ClBz-h_5 spectrum is in good agreement with previously published work;[11,12,14,24] however, there have been no extensive ClBz-d_5 REMPI or LIF spectra published to date to our knowledge. The overall appearance of the ClBz-d_5 spectrum is in reasonably good agreement with its non-deuterated analogue (see Figure 1) with the observation that the vibrational features in the ClBz-d_5 spectrum are generally red shifted compared to those in ClBz-h_5; there are, however, a range of differences in detail and these will be discussed below. The H/D isotopic shift of each vibration is clearly mode specific as participation of the hydrogen atoms is different – this will be more clearly seen in expanded spectral views presented later. If particularly large shifts occur, then these can lead to reordering of the vibrations and can also lead to different interactions between vibrations, depending on their proximity, symmetry, and efficiency of coupling.

As noted, although (1+1) REMPI spectra of both ^{35}Cl and ^{37}Cl isotopologues of each of ClBz-h_5 and ClBz-d_5 were recorded, only spectra of ClBz involving ^{35}Cl will be shown. The vibrational band positions of the ^{37}Cl isotopologues are given in Tables S1 and S2 of the Supplementary Material[39] for ClBz-h_5 and ClBz-d_5, respectively, where the (significantly smaller) isotopic effect owing to the chlorine atom can be observed. We shall occasionally refer to these shifts when discussing the assignment.

In the following, we shall tackle the assignments of the ClBz-h_5 and ClBz-d_5 spectra simultaneously. Our assignments are aided by previous work on ClBz-h_5 as well as the calculated vibrational frequencies, and use will also be made of previously-observed activity in corresponding spectra of FBz and toluene. To simplify the discussion we will separate the assignment into different wavenumber regions. As will be seen, most of the transitions in the region $\lesssim$ 1100 cm^{-1} can be assigned relatively straightforwardly; however, to higher wavenumber, there are regions of congestion, corresponding to progressions built on lower-wavenumber fundamentals, overtones, and combination bands. Hence assignments to higher wavenumber become less certain in the absence of other information (such as DF or ZEKE

spectra), and as a consequence we shall only provide assignments for key features, with some discussion of the other spectral features.

B. Calculated vibrational wavenumbers.

As noted above, the vibrations of benzene do not always clearly correspond to a calculated vibrational mode of a substituted benzene molecule unambiguously; as a consequence of this different Wilson labels have been used for the same vibration in different papers. Table 1 summarizes the different labels used in previous work together with the M_i label employed here. When discussing previous assignments, we will generally only employ the M_i nomenclature; if the reader wishes to cross-reference with a Wilson label from a previous work, use should be made of Table 1. The calculated vibrational wavenumbers for the S_0 states of ClBz-h_5 and ClBz-d_5 are presented in Table 2, where we also show experimental assignments from previous work. (For comparison, we show the calculated values for the ^{35}Cl and ^{37}Cl isotopologues of ClBz-h_5 and ClBz-d_5 in Table S3 of the Supplementary Material[39].)

1. *ClBz-h_5 S_0 state*

Our calculated B3LYP/aug-cc-pVTZ S_0 vibrational wavenumbers for ^{35}ClBz-h_5 (Table 2) are in very good agreement with the previous experimental results where an average deviation of ~1% from experimental results is observed. With regard to previous work (see Table 2), we note that there are a number of different calculated results presented in the work of Imhof and Kleinermanns[14]: the B3LYP/6-311G(d,p) values are in reasonable agreement with the present ones, particularly had these been scaled; the MP2/6-311G(d,p) results are variable, with some in better and some in poorer agreement with experiment than here (the value given for M_{18} is anomalous and it seems likely to be a typographical error); and the CAS(8,7) values are in significantly poorer agreement. Our previous results[9] employing the B3LYP/aug-cc-pVDZ level of theory can be seen to be in very good agreement with the present work, with the present values expected to be the more reliable since a larger basis set was employed. Assignments of the S_0 vibrations for ^{35}ClBz-h_5 have been discussed previously in ref. 9 and so are not discussed in great detail here: suffice to say that the assignments do not change.

A Duschinsky matrix expressing the ClBz-h_5 S_0 state vibrations in terms of those of the FBz-h_5 S_0 state is shown in Figure 2, and the same information is summarized in the last column of Table 1, where the occasional minor mixings of the M_i modes in ClBz can be seen, in stark contrast to the very mixed form of the vibrations when expressed as Wilson modes. The

largely diagonal nature of the Duschinsky matrix indicates that the normal modes of these species are largely the same, with a dominant (mixing coefficient ≥ 0.5) FBz-h_5 contribution present for every ClBz-h_5 mode; as such, each ClBz vibration can be associated with a particular M_i mode (mode diagrams are available in ref. 9). There are no previous S_0 results to compare to for the ^{37}ClBz-h_5 isotopologue; however, as the isotopic wavenumber shift is generally small (see Table S3 in the Supplementary Material[39]), and since our calculated values for ^{35}ClBz-h_5 proved to be in very good agreement with the experimental IR and Raman values, we are confident in their reliability.

2. *ClBz-d_5* S_0 *state.*

Figure 3 displays the ClBz-d_5 S_0 vibrational modes expressed in terms of those of ClBz-h_5 S_0, via a generalized Duschinsky rotation. The close-to-diagonal nature of the matrix suggests that the majority of the vibrations in ClBz-d_5 are very similar to those for ClBz-h_5 in the S_0 state; however, four pairs of significantly mixed vibrations occur – M_6/M_8, M_{17}/M_{18}, M_{25}/M_{26} and M_{27}/M_{28} – despite this, all thirty vibrational modes of ClBz-d_5 show a dominant contribution (coefficient ≥ 0.5), allowing all ClBz-d_5 vibrational modes to be numbered with the ClBz-h_5 labels, but with the proviso that these are mixed forms in a number of cases. To gain further insight into this, we have investigated how the ClBz-h_5 vibrational wavenumbers change as a function of the artificial mass of the hydrogen atoms as they all simultaneously change from 1 amu to 2 amu. This was achieved by calculating the harmonic vibrational frequencies for these artificial isotopologues, and producing plots of wavenumber against the mass of the 'hydrogen' atoms. Although not shown here, these showed very similar behaviour to that seen for fluorobenzene (see Figure 3 of ref. 30). For clarity in the following discussion, we employ M_i^d labels to designate the vibrational modes of a deuterated species, with the post-superscript (^{d}) indicating that we are referring to a vibration of the perdeuterated molecule in this case; the lack of such a superscript indicates that we are referring to the ClBz-h_5 isotopologue. For ClBz-d_5, no previous calculated values have been published to our knowledge, but good agreement is seen when comparing the ^{35}ClBz-d_5 calculated values (Table 2) to the experimental values of Nanney et al.[19], with an average deviation of 2%. No previous work seems to be available for the ^{37}ClBz-d_5 S_0 state. Calculated vibrational wavenumbers for all four ClBz isotopologues are presented in Table S3 of the Supplementary Material[39] for completeness.

3. S_1 *state*

The Duschinsky matrices illustrating how the S_1 state vibrations are expressed in terms of the S_0 ones, are presented in Figure 4 for both ClBz-h_5 and ClBz-d_5. It can be seen that a dominant (mixing coefficient ≥ 0.5) contribution is present for each vibration of each isotopologue, despite the changes in geometry and electronic structure that occur between the different electronic states. The S_1 vibrations are thus labelled with the same M_i (or M_i^d) label as in the ground state; we note that the M_8 vibration shows the most mixed character. Such significant mixing is not present in the deuterated isotopologue for M_8^d; however, here the M_{18}^d and M_{19}^d modes are significant mixtures of the corresponding S_0 modes. Although these are very mixed, we find that that the activity in the spectrum of ClBz-d_5 is very similar to that in ClBz-h_5; for example, the fairly prominent $(M_{19}^2)^d$ band is the analogue of the M_{19}^2 band between 530 and 600 cm^{-1} (see below), indicating that geometry changes as a result of the $S_1 \leftarrow S_0$ excitation are similar in both isotopologues. Of course, all other vibrations will have small admixtures of other vibrations of the same symmetry, but will largely resemble their dominant M_i designation.

In Table 3, we give the calculated TD-DFT B3LYP/aug-cc-pVTZ vibrational wavenumbers for the S_1 states of ^{35}ClBz-h_5 and ^{35}ClBz-d_5 (with the values for the ^{37}Cl isotopologues given in Table S3 of the Supplementary Material[39]). Our calculated ^{35}ClBz-h_5 B3LYP wavenumbers are in generally very good agreement with previous available experimental values by Jain and Bist,[6,7,8] Wright et al.,[24] and Imhof and Kleinermanns.[14] Somewhat poorer agreement is seen with the results of the CAS(8,7) calculations of ref. 14 – see Table 3 – as was the case for the S_0 state. We note here the peculiarity of the M_{14} mode, whose wavenumber was found to be very poorly calculated for FBz using the B3LYP/aug-cc-pVTZ method,[30] and this also seems to be the case here. Thus the assignment of this vibration rests on previous experimental work, previous calculated values using other methods for FBz,[29] and also the fact that there is no other reasonable assignment for the ClBz band associated with M_{14}^2 (see below).

There do not seem to be experimental values available for the S_1 state of the other isotopologues.

C. Assignment

1. *Low wavenumber range (0-530cm^{-1})*

(a) 0 – 450 cm^{-1}

Expanded views of the low energy regions of the ClBz-h_5 and ClBz-d_5 spectra are presented in Figure 5. In both spectra a strong origin band is observed with weaker features to higher wavenumber. Based on the calculated vibrational wavenumbers, comparison with previous spectra of ClBz and other monosubstituted benzenes, this low-wavenumber region is straightforwardly assigned. Bands at 286.0 cm^{-1} and 377.4 cm^{-1} are assigned as transitions to the b_2 symmetry fundamental mode, M_{30}, and the a_1 fundamental mode, M_{11}, respectively. There is very good agreement between those experimental fundamentals and our calculated B3LYP wavenumbers (Table 3). Additional weaker features are seen, including transitions to two overtone bands, M_{20}^2 and M_{14}^2, at 247.8 cm^{-1} and 407.6 cm^{-1}, respectively, and to a combination band of overall b_2 symmetry, $M_{14}M_{20}$, at 324.4 cm^{-1}; a few other small features appear to be hot bands or arise from ClBz-Ar complexes. The $M_{14}M_{20}$ band was not observed in the FBz spectrum[30] and it is weak in the present work; but as just noted, the overtones of both of its components are seen in both the present work, and this is also the case for FBz.[30] We have commented on the poor agreement between the experimental and the present calculated value for M_{14} above.

Regarding other studies on ClBz, the present spectrum represents a significant improvement over those previously available. In the absorption spectra of Bist and coworkers,[6,8] the M_{30}, M_{11}, M_{20}^2 and M_{14}^2 vibrations were observed, but not the $M_{14}M_{20}$ combination. The REMPI spectrum from Anderson et al.[11] is not shown below ~ 500 cm^{-1} and that of Murakami et al.[10] had a break in the spectrum in this wavenumber region, and hence none of the aforementioned four features are visible. The REMPI spectrum by Walter et al.[12,40] does appear to contain all four of these features, but these are not discussed nor assigned. A similar situation arises in the REMPI spectrum published by Wright et al.[24] where, although only the M_{30} and M_{11} features were assigned in this region, the cold spectrum reported in Figure 2(b) of that work does actually show all of the cold features assigned here.

The LIF excitation spectrum of Imhof and Kleinermanns[14] only show weak features attributed to the M_{30} and M_{11} modes, which were assigned, with DF spectra being recorded via these. These allowed confirmation of the assignment of these vibrations (albeit with a different nomenclature, see Table 1); participation of the chlorine atom is clearly different in different vibrational modes and it transpires that the isotope effect is significant for only a few transitions, with the M_{11} vibration experiencing the biggest shift of 5.0 cm^{-1} for ClBz-h_5.

Of note is that a weak feature ~4 cm^{-1} to lower wavenumber than the M_{11} feature was observed, which gave rise to a very similar DF spectrum.[14] Although it was not possible to rule out other possibilities, it was suggested that this weaker feature was due to the M_{11} vibration of the ^{37}ClBz-h_5 isotopologue and this is confirmed in the present mass-resolved work where the higher wavenumber feature appears in the ^{35}ClBz spectrum in Figure 5, while the weaker, lower-wavenumber feature appears only in the spectrum in the ^{37}ClBz mass channel (not shown, see Table S1 in the Supplementary Material[39]). Most other vibrational bands shift very little upon this isotopic change, for instance the M_{20}^2 and M_{14}^2 bands shift by only 0.4 and 0.2 cm^{-1}, respectively – see Tables S1 and S3.

The ClBz-d_5 spectrum of this region (inverted trace, Figure 5) demonstrates the same vibrational bands as ClBz-h_5 below 450 cm^{-1}; however, significant shifts upon deuteration are seen, most notably in the $(M_{14}^2)^d$ vibrational band, which shifts by ~54 cm^{-1} and as a consequence appears to lower wavenumber than the M_{11}^d band; other vibrations shift by only a small amount. These observations are consistent with the corresponding spectra of FBz-h_5 and FBz-d_5.[30] Again, very small shifts are seen between the ^{35}Cl and ^{37}Cl isotopologues of ClBz-d_5, with the largest change again being for the M_{11} vibration, amounting to 4.8 cm^{-1} for ClBz-d_5.

(b) >450 cm^{-1}

Just above 500 cm^{-1}, a pair of bands in the ^{35}ClBz-h_5 REMPI spectrum appears. These were assigned as transitions to a Fermi resonance by Cvitaš and Hollas[5] involving the M_{29} fundamental and the $M_{14}M_{20}$ combination band (both of b_2 symmetry); Jain and Bist[8] confirmed this as a Fermi resonance (FR), but reassigned the interacting combination to $M_{14}M_{19}$, with which we concur. Vibrations that contribute to a FR are each called zero-order states (ZOSs), which interact to form vibrational eigenstates, sometimes called Fermi resonance components. A FR is strictly an interaction between two ZOSs; however, more than two states can interact, and this is termed a complex Fermi resonance. The FR assignment of these two bands was confirmed in DF,[14] REMPI-PES[21], ZEKE[24] and MATI[26] spectroscopic studies, where the spectra suggest that the lower wavenumber component at 520.6 cm^{-1} has a majority contribution from the M_{29} ZOS, while the band appearing at 524.2 cm^{-1} has a majority contribution from the $M_{14}M_{19}$ ZOS. In the following, we shall refer to this pair of features as M_{29}^{FR} for conciseness, and have labelled it as such in Figure 5. This feature appears as an essentially identical doublet in the ^{37}ClBz-h_5 mass channel (not shown), in line

with the calculated vibrational wavenumbers, which suggest each feature should move by only ~0.1 cm^{-1}; clearly the changes in the FR coupling are small enough not to be discerned at our resolution.

It is notable that this FR is not observed in the ClBz-d_5 spectrum (inverted trace, Figure 5). This is easily understood, since the contributing ZOSs have shifted in wavenumber: the M_{29}^{d} band is seen at 501.8 cm^{-1} while the $(M_{14}M_{19})^{d}$ band may be attributable to a very weak feature at 446.6 cm^{-1}.

A weak feature to slightly lower wavenumber of the M_{29}^{FR} and M_{29}^{d} features may be seen in the spectra of each isotopologue, which corresponds to transitions to the third overtone of the M_{20} vibration, M_{20}^{4} and $(M_{20}^{4})^{d}$.

Assignments and wavenumbers are given in Tables 4 and 5 for the spectra of ClBz-h_5 and ClBz-d_5, respectively.

2. *Medium wavenumber range (530 – 1120 cm^{-1})*

The next spectral range to be discussed in detail shows bands arising from transitions to overtones and combinations of vibrations already assigned, as well as new fundamental bands which not only dominate this wavenumber region, but also give rise to overtones and combination bands which are prominent to higher wavenumber. The expanded spectra over this region for ClBz-h_5 and ClBz-d_5 can be seen in Figure 6. The assignment shown is based upon both the experimental values for the lower wavenumber fundamentals, discussed above, and in cases where these are not available then we use the calculated frequencies that are given in Table 3; in the case of ClBz-h_5, previous work has also aided the assignment. To confirm the assignments we also examined the shifts upon deuteration, comparing these to the calculated ones (Table 3) as well as $^{35}Cl/^{37}Cl$ isotope shifts (see Tables S1 – S3 of the Supplementary Material[39]) when assigning the bands.

(a) 530 –700 cm^{-1}

In previous work, this wavenumber region of the spectrum has been reported,[12,24] but these spectra were not of very high quality (this spectral range was omitted in the scan of ref. 14). In the present ClBz-h_5 spectrum (Figure 6, upper trace) there is a group of bands in the 600 – 700 cm^{-1} range, which consists of three main features at 639.4, 671.6 and 681.2 cm^{-1} as well as a number of weaker features. Comparing with the calculated vibrational wavenumbers, as well as the corresponding spectra of FBz and toluene, it is highly likely that one of the more-

intense features is attributable to the M_{10} vibration. We might initially also have expected to see the $M_{18}M_{19}$ combination band, which is seen to be in Fermi resonance with the M_{10} vibration in both toluene and FBz; however, the M_{10} vibration is more mass-sensitive to the change in the mass of the substituent than those two vibrations, and so has moved to significantly lower wavenumber in ClBz than the $M_{18}M_{19}$ combination, and so the latter band, not being inherently bright, does not appear. However, it might be that transitions to the overtones of the contributing vibrations do appear, and although the M_{18}^2 band is expect to appear at significantly higher wavenumber, M_{19}^2 is plausible. A good approximation to the experimental value of M_{19} can be obtained from the average wavenumber of M_{29}^{FR}, one ZOS of which is $M_{14}M_{19}$, since these two features are very close in wavenumber. The mean value of the two FR components is 522.4 cm^{-1}, and so knowledge of the wavenumber of the M_{14}^2, seen lower in wavenumber, allows the M_{19} vibrational wavenumber to be deduced as ~320 cm^{-1}, and hence the M_{19}^2 transition is most likely responsible for the band at 639.4 cm^{-1}. In toluene and FBz, the M_{10} vibration has been concluded to be bright, and so should be quite intense here, and seems likely to be the band at 671.6 cm^{-1} based on the very good agreement with the calculated wavenumber. We shall come back to the third feature at 681.2 cm^{-1} shortly.

We now consider the similar region of the spectrum of ClBz-d_5, which also contains three bands between 530–660 cm^{-1}, with the third being part of the region labelled α^d in Figure 6 (see expanded view in that figure). Looking at the expected values for the same vibrations, again based on the available experimental overtones, combinations and calculated values, it seems most reasonable to assign the band at 536.4 cm^{-1} to the $(M_{19}^2)^d$ transition and the band at 650.4 cm^{-1} to M_{10}^d. These assignments fit the calculated shifts upon deuteration, as well as the ^{35}Cl/^{37}Cl shifts, where in the latter case the M_{19} overtone essentially does not shift upon Cl-isotope change, while the M_{10} vibration undergoes a 1–2 cm^{-1} red shift. As with ClBz-h_5, there is a third feature (at 570.6 cm^{-1}) in Figure 6 that is not straightforward to assign. Given that geometry changes between the two isotopologues are expected to be similar, we might expect similar vibrational activity, particularly if the vibrations involved are not strongly mass-sensitive. Considering the vibrational wavenumbers for the ClBz-h_5 and ClBz-d_5 isotopologues, then possible assignments are transitions to the $M_{14}M_{18}$ and $(M_{14}M_{18})^d$ combinations (b_2 symmetry and so vibronically-allowed), and $M_{17}M_{20}$ and $(M_{17}M_{20})^d$ (a_1 symmetry). Neither a ZEKE nor DF spectrum has been recorded via these features yet, and so initially it is difficult to decide between these, given that one component in each case is based

solely on a calculated value; particularly since the shifts upon deuteration are extremely similar; in addition, the ^{35}Cl/^{37}Cl shifts are expected to be small in both cases, which is consistent with essentially no shift in the experimental features. A provisional assignment for these features comes from noting that the corresponding spectrum of FBz[28,30] contains a feature due to M_{17}^2 and we find a feature at 1113.8 cm^{-1} that matches the expected position for this (see later). This then gives a very good agreement with the 570.6 cm^{-1} feature arising from $M_{17}M_{20}$; further, the corresponding $(M_{17}M_{20})^d$ feature also appears in the expected position for ClBz-d_5, based on the identification of $(M_{17}^2)^d$ – see later.

We note that if this assignment is correct then it may be that this vibration is in Fermi resonance with the M_{10} vibration for ClBz-h_5, and so evidence for this would be seen in the vibrational activity in ZEKE or DF spectra. (In contrast, if $M_{14}M_{18}$ were the correct assignment, no such interaction would occur, owing to the different symmetries.) We note that there are other weak features close to the expected bright ZOS, M_{10}^d –see expanded view of region α^d in Figure 6, some of which may be in Fermi resonance, for which suggested assignments are given in Table 5.

(b) 700–975 cm^{-1}

There is an interesting set of weak features in the 700–750 cm^{-1} region for ClBz-d_5, and an expanded view of this region is shown in Figure 6, labelled β^d. These have an almost identical appearance and wavenumber in the ^{35}ClBz-d_5 and ^{37}ClBz-d_5 spectra (not shown), ruling out combinations involving the M_{11}^d vibration for the main features. Suggested assignments of the bands in region β^d are shown in Figure 6 and Table 5; we note that there is no corresponding set of features in ClBz-h_5. Such small differences in weak features between the spectra of the isotopologues are likely attributable to small changes in vibrational wavenumbers and transition strengths and hence slightly different Franck-Condon factors (FCFs).

Although weak, the next features of interest are located in the range 850 – 910 cm^{-1} in the ClBz-h_5 spectrum – and there are also weak features in the ClBz-d_5 spectrum to slightly lower wavenumber. These turn out not to be easy to assign and we give our best attempt at this in Tables 4 and 5 after examining the possible assignments and observed isotopic shifts.

We now move onto the bands at 932.2 and 964.8 cm^{-1} that are assigned as transitions to the M_8 and M_9 fundamentals, respectively. Note that the wavenumber ordering of these vibrations

in the S_1 is reversed from that in the S_0 state, as was seen for FBz[30] and toluene.[34] (Note that a few weak features have been attributed to the ClBz-Ar complex, and these have been indicated with "Ar" in Figure 6.) Transitions involving these vibrations dominate the spectrum recorded for ClBz-h_5 in this wavenumber region and these two vibrations, along with M_{29}^{FR}, make a contribution to many of the combination and overtone transitons that are seen in the higher wavenumber region. The $^{35}Cl/^{37}Cl$ shift for the M_8 and M_9 vibrations is calculated to be within our experimental precision, in line with the observations in the spectra. These vibrational levels have been used as intermediate states in REMPI-PES experiments by Asselin et al.,[21] ZEKE experiments by Wright et al.[24] and also DF spectra from each of these two levels have been reported by Imhof and Kleinermanns;[14] discussion of these previous studies will be presented later, in Sections D2(b) and D3(b).

We now move onto considering the corresponding region of the spectrum for ClBz-d_5. The M_8^d vibration is calculated to have a significant red shift (~149 cm^{-1}), and an assignment of the band at 783.2 cm^{-1} is made based on this expected shift and by comparison with the spectra of the corresponding isotopologues for FBz.[30] The M_9^d band has undergone a much smaller isotopic red shift (~39 cm^{-1}) and is the intense band at 926.2 cm^{-1}. It is interesting to note that the M_8^d band is much weaker than the M_8 one. We note that for ClBz-h_5 the M_8 and M_9 vibrations become heavily Duschinsky mixed in the S_1 state, while this occurs to a much lesser extent in ClBz-d_5. We conclude from this that it is a geometry change along the M_9 coordinate that gives the main contribution to the intensity for these vibrations, and the mixed nature of the M_8 and M_9 modes in ClBz-h_5 leads to both being intense, while in ClBz-d_5 the significantly weaker mixing means the M_9^d band is far more intense than the M_8^d one. Further comments on these ClBz-h_5 bands will be made below. In passing, we note that a weak band at 973.0 cm^{-1} has no obvious overtone/combination band assignment and so is tentatively assigned to M_{28} on the basis of the calculated wavenumber.

In the ClBz-d_5 spectrum, just before the M_9^d band, there is a feature at 913.4 cm^{-1} that is initially difficult to assign. On the basis of the expected wavenumber, several candidates are possible. Although initially-likely candidates such as $(M_{11}M_{19}^2)^d$, and $(M_{11}M_{30}^2)^d$ are tempting, particularly since their components appear in the spectrum earlier on, in fact we find that the 913.4 cm^{-1} feature is essentially insensitive to $^{35}Cl/^{37}Cl$ isotopic change – see the expanded view on the bottom right of Figure 6. A possible assignment of this feature is the $(M_{17}^2)^d$ transition, which was also observed in corresponding spectrum of FBz-d_5.[30] This vibration is not expected to shift appreciatively upon $^{35/37}Cl$ substitution as observed, and this

the suggests a M_{17}^{d} wavenumber of 456.7 cm^{-1}, which compares very favourably with the calculated value of 455.0 cm^{-1} and we thus assign the 913.4 cm^{-1} feature as $(M_{17}^{2})^{d}$. It is possible that this vibration is in Fermi resonance with M_{9}^{d} at 926.2 cm^{-1}; ZEKE or DF spectra would be able to confirm whether this is the case or not. With this assignment, it was then possible to find a band that could be assigned to the corresponding M_{17}^{2} transition in the ClBz-h_5 spectrum at 1113.8 cm^{-1} – this was also observed in FBz-h_5.[28,30] As noted earlier, the assignment of these transitions allowed the identification of the $M_{17}M_{20}$ and $(M_{17}M_{20})^{d}$ features lower in wavenumber.

(c) Regions γ and γ^{d}

Next we consider the region of the ClBz-h_5 spectrum labelled as γ in the top trace of Figure 6, which has an analogous region in the ClBz-d_5, labelled γ^{d}; expanded views of these spectral regions are given in Figure 7, where both the corresponding ^{35}Cl and ^{37}Cl traces are given in each case. The assignment of these regions proves not to be completely straightforward, but is helped significantly by being able to compare the spectra of the four isotopologues and also by analogy with the FBz[28,30] and toluene[34] spectra. From the latter two studies, together with the experimental and calculated vibrational wavenumbers, we would expect to find features corresponding to the $M_{10}M_{11}$ combination band and the M_6 vibration in this region of the spectrum. These have been found to be "bright" in the case of toluene using time-resolved photoelectron spectroscopy in combination with ZEKE spectroscopy,[34] and have also been observed for FBz.[28,30] These are hence expected to be relatively intense here, but may be in Fermi resonance with other features. Also at this wavenumber are expected to be features arising from the the two overtones and the combination that occur from the M_{29}^{FR} overtone components, as well as the single $(M_{29}^{2})^{d}$ band in the case of ClBz-d_5. Other combinations and overtones may also appear, particularly if they occur close to bright ZOSs and hence gain intensity from them via Fermi resonance. With these points in mind, we commence by looking at the ClBz-h_5 spectrum. First, we note that the M_6 vibration was calculated to be a few tens of cm^{-1} too low for FBz[30] and this being the case here, we would expect the M_6 to appear at ~ 1060 cm^{-1}, which is consistent with the band at 1066 cm^{-1} being associated primarily with M_6. Further, this band is seen to shift slightly to the red for ^{37}ClBz-h_5 (see Figure 7), consistent with expectations based on the calculated isotopic shift, and bearing in mind that this vibration is likely to be in Fermi resonance. (Being in FR can affect both its expected position and the extent of its isotopic shift – here, mixing with a combination

containing M_{11}, for example, may exacerbate the shift, as seems to be the case.) Note that we have already determined values for M_{10} and M_{11} and hence we can expect the $M_{10}M_{11}$ combination band at ~1049 cm^{-1}. Given anharmonicity and a potential Fermi resonance with the M_6 vibration, the band at 1043.0 cm^{-1} is a reasonable match to this expected position; additionally, upon $^{35/37}$Cl substitution, a shift of ~ 6 cm^{-1} occurs, consistent with the involvement of the M_{11} vibration (see Figure 7). The assignment of the major contributors to the two most intense bands in this region thus seems relatively secure; as will be noted later, these assignments are also in line with previous ZEKE and REMPI-PES work.

With regards to the other features in this region, we note that the $(M_{29}^{FR})^2$ features, M_{29}^2, $M_{14}M_{19}M_{29}$ and $M_{14}^2M_{19}^2$ are expected at ~ 1041, 1044 and 1047 cm^{-1}, respectively; additionally, in the ^{37}ClBz-h_5 spectrum the M_{29}^2 and $M_{14}M_{19}M_{29}$ components are expected to separate from the $M_{10}M_{11}$ band. Since these components are of a_1 symmetry they are not vibronically allowed, but could either have inherent intensity or could gain intensity from FR, with the interaction with the $M_{10}M_{11}$ being the most likely. The M_{29}^2 and $M_{14}M_{19}M_{29}$ components are the closest in wavenumber and so are the most likely to interact with $M_{10}M_{11}$, and so contribute to the 1043.0 cm^{-1} feature. We thus conclude that the band at 1043.0 cm^{-1} in the ^{35}ClBz-h_5 spectrum comprises three overlapped features, and we shall come back to this point later. Finally, we note that there are two other weak features in this region. The band at 1057.8 cm^{-1} in the ^{35}ClBz-h_5 spectrum may be assigned to a transition to the $M_{11}M_{17}M_{20}$ combination, i.e. M_{11} plus the $M_{17}M_{20}$ combination discussed earlier; and the band at 1017.0 cm^{-1} can be assigned to $M_{11}M_{19}^2$. Both of the latter two bands, containing a contribution from M_{11}, are observed to shift in line with expectations upon $^{35/37}$Cl substitution (Figure 7).

With regard to the γ^d region of the ClBz-d_5 spectrum, we clearly expect transitions to both $(M_{10}M_{11})^d$ and M_6^d to be present as these are bright ZOSs. Based on the experimental values for M_{10}^d and M_{11}^d, we expect the combination band to appear at ~ 1020 cm^{-1}, which would be consistent with the band at 1017.0 cm^{-1} in the ^{35}ClBz-d_5 spectrum; further, there is a feature in the ^{37}ClBz-d_5 spectrum at about the correct red shift for this vibration (see Figure 7). We also note that, based on the value of M_6 for ^{35}ClBz-h_5 and the calculated isotopic shift upon deuteration, the band at 1032.6 cm^{-1} likely arises mainly from M_6^d; again, it shows a small red shift in line with expectations. The assignments of the two features at 983.4 and 1001.4 cm^{-1} are rather less clear. The latter is consistent with the expected position of $(M_{29}^2)^d$ but apparently shows a significant shift more in line with having a contribution from M_{11}^d (Figure 7). With that in mind, we looked for a combination involving the latter, and found that the

($M_{11}M_{14}M_{17}$)^d vibration matched the observed wavenumber very well; we also then identified a band at 633.6 cm^{-1}, which fits the expected position of ($M_{14}M_{17}$)^d. Even more suggestive that this is a plausible assignment is that the band at 983.4 cm^{-1} is at the correct wavenumber to be ($M_{14}^3M_{17}$)^d – i.e. the observed (M_{14}^2)^d overtone in combination with ($M_{14}M_{17}$)^d; further, this vibration is not expected to undergo a $^{35/37}$Cl shift, as observed for this band. We note that the 983.4 and 1001.4 cm^{-1} assignments are to vibrations that have b_2 symmetry and hence potentially could be in Fermi resonance. We briefly return to the band at 1001.4 cm^{-1} which we noted could have contributions from (M_{29}^2)^d; in the ^{37}ClBz-d_5 spectrum there are other weak features close to this wavenumber, one of which could be attributed to this vibration, in line with there being overlapped (M_{29}^{FR})^2 features in ClBz-h_5.

3. *High wavenumber range (1120- 3000 cm^{-1})*

This wavenumber region of the ClBz-h_5 and ClBz-d_5 spectra becomes much richer in structure, particularly from ~1800 cm^{-1} onwards. It includes numerous intense features and an increasing number of relatively weak bands – see Figure 1. In the ClBz-h_5 spectrum, it is possible to identify pairs of bands that arise from combinations involving both M_8 and M_9, and a number of these are labelled in Figure 1, as well as being included in Table 4. It is then seen that the same combinations are seen in ClBz-d_5 although here only those involving the M_9^d vibration are immediately obvious, as these are much more intense than the M_8^d ones, in line with the observed intensities for the fundamentals (see above, and Figure 6).

In the ClBz-h_5 spectrum there are a number of weak features from ~1120–1400 cm^{-1} which are not straightforward to assign. It is possible to come up with likely assignments for the more-intense bands, based on expected wavenumber and isotopic shifts: as an example, we note that the features between 1200-1260 cm^{-1} are expected to include contributions from M_8M_{30} and M_9M_{30}, and the $^{35/37}$Cl shifts of ~ 2 cm^{-1} are consistent with these assignments. Clearly, however, there are many other weaker contributions in this region, but a comprehensive assignment of these is largely a thankless task.

Some features are quite striking; for example, the pair of features between 1450–1500 cm^{-1} are almost certainly transitions to the M_{29}^{FR} components in combination with the M_8 and M_9 bands, since each feature is split (consistent with containing contributions from M_{29}^{FR}) and also these show almost no $^{35/37}$Cl shift. Between ~1700–2000 cm^{-1}, a set of bands are present at 1865 cm^{-1}, 1898 cm^{-1} and 1931 cm^{-1} that match well the expected positions of M_8^2, M_8M_9 and M_9^2 transitions, to which these are assigned, respectively. It is interesting to note

that the M_8^2 band is much weaker than the M_9^2 band, with the M_8M_9 combination band being the most intense. In the range 1970 –2015 cm^{-1} there are bands that can be attributed to transitions to the combination bands, $M_8M_{10}M_{11}$ and $M_9M_{10}M_{11}$, as well as M_6M_8 and M_6M_9. These main features do not demonstrate a significant $^{35/37}$Cl shift (as expected for the suggested assignments), but there are other bands here that do, and so clearly there are more contributions here than those highlighted. We have indicated some of the more secure assignments in Figure 1 and in Table 4 for ^{35}ClBz, with the ^{37}ClBz analogues in Table S1. As we move up in wavenumber, the prominent bands become surrounded by weaker and congested features, suggesting complex Fermi resonances.

When we look at the ClBz-d_5 spectrum, it is less straightforward to pick out features since the clear pairing of features seen for the M_8 and M_9 combination bands in ClBz-h_5 is not present for M_8^d and M_9^d in ClBz-d_5. However, guided by the ClBz-h_5 assignment and the wavenumber values obtained from the lower region of the spectrum, it is possible to identify combinations of key features with M_6^d, M_9^d and M_{29}^d and again these are indicated in Figure 1, as well as in Table 5 for ^{35}ClBz-d_5, with the ^{37}ClBz-d_5 analogues in Table S2.

D. Discussion of previous photoionization and DF studies

We shall now discuss previous DF and photoionization studies, with the latter falling into conventional HeI photoelectron spectroscopy, REMPI-PES, ZEKE and MATI studies. For the photoionization studies, it will be necessary to discuss vibrations of the cation and so we comment on their labelling first.

1. *Vibrational Labelling for ClBz-h_5^+*

First of all, we note that the Duschinsky matrix (see Figure 8a) shows that the $\tilde{X}\ ^2B_1$ state of the ClBz-h_5^+ cation, denoted D_0^+, has vibrational modes that each have a dominant contribution (mixing coefficient ≥ 0.5) from the corresponding M_i mode when expressed in terms of the vibrations of the S_0 state. As a consequence, we can use the M_i labels, but noting that the cation vibrational motions will not be identical. For clarity in the discussion, we append a post-superscript + to each label, viz. M_i^+. In Table 6, we give the calculated vibrational wavenumbers for the ground state ^{35}ClBz-h_5^+ and ^{35}ClBz-d_5^+ isotopologues and also include both experimental and theoretical values from previous work. Note that in the following, we have inferred which M_i^+ mode was being referred to in previous work, from the wavenumber values. Again, most workers have made use of the Wilson labels, but the

inconsistent assignment of these makes it difficult to discuss the observed activity; in particular, since the assignment of the cation vibration in resonant experiments is often dependent on the identified vibrational level in the intermediate state (or vice versa). We note that in the ZEKE study of ref. 24, the calculated vibrational wavenumbers were given in terms of both Mulliken and Wilson labelling; however, it should be noted that although the Mulliken label numbers are the same as the M_i labels in most cases for ClBz-h_5, in fact M_6 is ν_7 and M_7 is ν_6 (see ref. 9). We also recall that the M_8 and M_9 vibrations in the S_1 state have the opposite wavenumber order to that in the S_0 state, and this has led to these vibrations being misnumbered, for example those of the S_1 and D_0^+ states in ref. 24. Duschinsky matrices (not shown) confirm that the M_i^d labels can be used for ClBz-d_5.

2. *Previous resonant photoionization work on ClBz-h_5*

We first discuss the previous multiphoton photoionization studies in the light of the assignments above, which will also provide insight into the labelling of the cation vibrations. We break the discussion into wavenumber regions, or sets of features, of the S_1 state. We shall then consider the two one-photon studies.

(a) Low wavenumber features 0-530 cm^{-1}

Anderson et al.[11] recorded REMPI-PES spectra via the S_1 origin, M_{30}, M_{11} and M_{29} levels. Because of the low resolution, it is not always clear which vibrations they observed via these different levels, and it is also not clear which of the M_{29}^{FR} components they excited. Hence, in Table 6 we emphasise the wavenumbers and assignments from the more reliable ZEKE[24] and MATI[26] spectra, which mostly concur with the REMPI-PES results of Asselin et al.[21]

We also note that Asselin et al.[21] recorded REMPI-PES spectra of ClBz-d_5 through the S_1 origin and M_{11}^d levels, leading to the observation of progressions of 413 cm^{-1}, assigned to M_{11}^{d+}, which is in good agreement with the calculated value obtained here (Table 6). Also a combination band at 1171 cm^{-1} was tentatively assigned as involving the M_{11}^{d+} vibration, which would allow another a_1 fundamental vibration of ~760 cm^{-1} to be derived, our best suggestion for this vibration would be M_8^{d+} (Table 6).

(b) M_8 and M_9 bands

Care is required when discussing the vibrations in ClBz-h_5 that give rise to the two features at 932.2 and 964.8 cm^{-1} in the REMPI spectrum because of their mixed nature (see above). These vibrations have switched order from that in the S_0 state – a phenomenon also seen for FBz.[28,30] It thus needs to be noted that in the ZEKE study[24] the Mulliken ordering in the S_1 state gives an incorrect association of the labels, based on the dominant vibrational motion, compared to that in the S_0 state; in the following we shall use the M_i labels. In the ZEKE study, the identity of the intermediate ~965 cm^{-1} feature as M_9 (labelled ν_8 therein) was apparently clear, since, when exciting via this level, there was a very strong $\Delta v = 0$ band observed, corresponding to M_9^+, together with the M_{11}^+ fundamental and the $(M_9M_{11})^+$ combination band (the latter was part of a doublet, with the partner being assigned as M_5^+). Interestingly, when exciting via the lower wavenumber M_8 level at ~932 cm^{-1} (labelled ν_9 therein), two ZEKE bands of very similar intensity were observed, and assigned as M_8^+ and M_9^+; this intermediate vibrational level was thus assigned as the M_8 vibration, but the observation of two strong components was taken as implying this level had mixed character in the S_1 state, although this does not explain the observation of the single band when exciting via the ~965 cm^{-1} feature. We note that the latter does not fit in with the appearance of the Duschinsky matrix for the S_1 and D_0^+ vibrations (Figure 8b), which suggests that these vibrations are of very similar forms in the S_1 and D_0^+ states. Based on the ZEKE intensities, we might expect M_9^+ to have a motion very similar to that of M_9 in the S_1 state, and M_8^+ to be a mix of the S_1 M_8 and M_9 motions (i.e. a similar situation as that between the S_0 and S_1 states); so, either the present calculations are misleading, or another explanation will need to be found for the observed behaviour. So, for example, if these states did mix to some extent during the $D_0^+ \leftarrow S_1$ ionization and if the M_9 vibration has a significantly higher photoionization cross section than does the M_8 vibration, then this could go some way to explaining the observed spectra.

The observation of M_5^+ in the ZEKE spectrum[24] when exciting through M_9 is interesting, although we note that the motions of these vibrations are quite similar;[9] as a consequence, this can be rationalized via the geometry change upon ionization. Lembach and Brutschy[26] did not excite via these levels in their MATI study, but Asselin et al.[21] and Walter et al.[12] did, but the resolution was not sufficient to observe the closely-spaced bands noted above.

(c) Region γ

We have discussed the assignment of Region γ in the ClBz-h_5 REMPI spectrum (see Figures 6 and 7) above, where we suggest that the two bands at 1043.0 and 1066.0 cm^{-1} have major contributions from $M_{10}M_{11}$ and M_6, respectively. The former was also noted as probably containing contributions from the overtone region of M_{29}^{FR}, viz. M_{29}^2, $M_{14}M_{19}M_{29}$ (and perhaps $M_{14}^2M_{19}^2$).

ZEKE spectra were recorded[24] via each of these two features and some common activity was seen in both. When exciting via the 1066 cm^{-1} level, three intense bands were observed at 718 cm^{-1}, 1120 cm^{-1} and 1147 cm^{-1}, with the latter two being the most intense, and the 1147 cm^{-1} slightly the greater. When exciting via the 1042 cm^{-1} feature (denoted א in ref. 24), the 1120 cm^{-1} band still appeared, albeit not as intensely, with the 1147 cm^{-1} band now being somewhat weaker; additionally, the 718 cm^{-1} band was very intense. Thus, the M_6 and $M_{10}M_{11}$ vibrations appear to be in FR in the S_1 state (as well as possibly in the cation) and it is interesting to note that the M_6 and $M_{10}M_{11}$ vibrations are also in Fermi resonance in the S_1 state of FBz[28] and also in toluene-h_8.[34]

These observations led to some uncertainty in deciding on the assignment of these ZEKE features, although the assignment of the S_1 state features was consistent with that here; namely, the 1042 cm^{-1} band was $M_{10}M_{11}$ (with likely contributions from $(M_{29}^{FR})^2$ components, and the 1066 cm feature was ν_7 (we recall that we have noted previously[9] and above, that the wavenumber ordering of the M_6 and M_7 modes in ClBz are switched compared to FBz; hence, the ν_7 designation in ref. 24 is actually M_6). Indeed in the text of ref. 24 the impression is given that the 1147 cm^{-1} ZEKE band is assigned to M_6^+, and this is consistent with Figure 8a in that work, while in Table III of that work it is the ~1120 cm^{-1} (1116 cm^{-1} in the table) feature that is assigned to this mode; elsewhere in the text the difficulty in deciding between these two assignments is noted. The derived wavenumbers for M_{10}^+ and M_{11}^+ suggest the combination band $(M_{10}M_{11})^+$ should be at ~ 1140 cm^{-1} and thus be associated with the 1147 cm^{-1} ZEKE feature. We note here that our calculated values of M_{10}^+ and M_{11}^+ agree very well with the ZEKE values, and so support the assignment of the 1147 cm^{-1} band to $(M_{10}M_{11})^+$; further, our calculated value for M_6^+ would be consistent with the assignment of the 1116 cm^{-1} band to M_6^+; the difference between the calculated and the experimental value for the M_6^+ vibration is then in line with the differences observed for the corresponding neutral in the S_1 state in both ClBz (Table 3) and FBz (ref. 30). This

assignment is the same as Kwon et al.,[25] and other workers who have previously assigned the vibration at ~1120 cm^{-1} to the M_6^+ vibration.[21,26]

The above suggests that the ZEKE intensities in ref. 24 are not immediately representative of the originating resonant level (as was commented on for ZEKE spectra via M_8 and M_9 above), and suggests other factors may be at play, such as wavenumber-dependent photoionization cross sections, or other photophysical processes.

The ZEKE spectrum recorded through the 1042 cm^{-1} band[24] also exhibited bands due to $(M_{29}^2)^+$ and $(M_{14}M_{19}M_{29})^+$, confirming that this consists of a number of overlapped features, which were excited simultaneously and/or are in Fermi resonance, noting that weak features attributable to $(M_{29}^2)^+$ and $(M_{14}M_{19}M_{29})^+$ also seem to appear in the ZEKE spectrum excited via the 1066.0 cm^{-1} level. It would be interesting to record ZEKE spectra at various points through Region γ and to try and disentangle the contributions; also of interest would be picosecond time-resolved photoelectron spectra. Corresponding experiments on ClBz-d_5 across the γ^d region would also be useful.

Lastly, we note that in the two-photon excitation REMPI studies by Murakami et al.[10] the spectrum is dominated by a feature at 1564 cm^{-1}, which is assigned to Wilson mode ν_{14} therein. Interestingly, this mode does not appear with any great intensity in the present one-photon excitation spectrum (the agreement between the wavenumber of observed features in ref. 10 and here is such that the 1564 cm^{-1} feature is none of those noted in Table 4). This differing intensity lies in one- and two-photon transition strengths, as discussed in refs 10 and 41. According to previous work (see Table 1), this mode should be M_{25} or M_{26}, with the description of the mode as[10] a "Kekulé-type bond alternating C-C stretching vibration" suggesting M_{25} (see Fig. 5 of ref. 9). The experimental wavenumber does not compare well with any of the calculated wavenumbers (Table 3), however.

(d) One-photon photoionization studies

In 2002, Kwon et al.[25] recorded a one-photon MATI spectrum of ClBz-h_5, for both ^{35}Cl and ^{37}Cl isotopologues. Their wavenumbers for the various M_i^+ vibrations are given in Table 6, and these are mostly in very good agreement with previous work. We have omitted their value of 1411 cm^{-1} for the M_5^+ vibration as it does not agree well with either the ZEKE value, nor the calculated value. Their other suggestion for this band, which seems to correspond to $(M_9M_{11})^+$, seems to fit the calculated and previous experimental values better. We note that

their values for M_{19}^+ (482 cm^{-1}) and M_{30}^+ (286 cm^{-1}) are discrepant compared to previous values, but these were very weak and so possibly misassigned; these have been included in Table 6, but we have indicated our qualms regarding these values. It is worthwhile comparing these one-colour MATI spectra to the older, conventional HeI PES spectra of Potts et al.[22] who analysed vibrational structure in the first photoelectron band, yielding vibrational wavenumbers of 417, 1112 and 1460 cm^{-1}, which are assignable to M_{11}^+, $(M_{10}M_{11})^+$ and, plausibly, the M_5^+ or $M_8M_{29}^{FR}$ vibrations, although the 1460 cm^{-1} band might also be assignable to $(M_9M_{11})^+$, similar to the Kwon et al. 1411 cm^{-1} band, given the likely error in the HeI PES vibrational spacings. Overall, the appearance of the early part of the HeI spectrum (see Figure 1(b) of ref. 22) is reassuringly similar to that of the MATI spectrum (see Figure 2(a) of ref. 25).

3. *Previous dispersed fluorescence work on ClBz-h_5*

(a) Low wavenumber region

Imhof and Kleinermanns[14] have recorded a range of DF spectra of ClBz from various S_1 vibrational levels that correspond to those discussed herein, and from which ZEKE spectra have been recorded. In each case, the assignment of the S_1 vibrational level should be evident from the vibrational structure seen for the S_0 state from DF spectroscopy, and will now be discussed. As we will show below, although the DF spectra recorded from low wavenumber features in the S_1 state of ClBz-h_5 are largely consistent with the assignments from the photoionization studies and those discussed above, those from higher wavenumber features are not.

First we note that DF spectra recorded via the origin largely show activity in S_0 a_1 vibrations, with the most intense band arising from the M_9 vibration, in agreement with the DF spectrum of FBz via the origin.[28] Also seen is the b_2 mode, M_{29}, which was also observed, although much more weakly than in the DF spectra of FBz.[28] When dispersing from the M_{30} band, the $\Delta v = 0$ propensity rule is obeyed and an intense band corresponding to the ClBz ground state M_{30} vibration is also seen, confirming the assignment, and in agreement with the observations in the ZEKE spectrum.[24] DF spectra were also recorded via two bands at 384 and 380 cm^{-1}, which were extremely similar, and assignments were made to the ^{35}ClBz-h_5 and ^{37}ClBz-h_5 S_1 M_{11} modes (recalling that this mode is particularly sensitive to the mass of the chlorine atom). These authors also reported DF spectra via each component of M_{29}^{FR}. In agreement with the

REMPI-PES spectra of ref. 21, the MATI spectrum of ref. 26, and the ZEKE spectra of ref. 24, they also confirmed that the lower component arose from the eigenstate with more M_{29} character, while the upper one had more of the $M_{14}M_{19}$ combination. (In FBz, this Fermi resonance does not exist.[28,30])

(b) M_8 and M_9

The picture was far from straightforward when looking at the DF spectra from the two levels at 932.2 and 964.8 cm^{-1} (cited at 934 and 966 cm^{-1} in ref. 14) and the authors commented on this, eventually suggesting significant mixings between vibrations to account for their observations.[14] However, we note that some suggested mixings, such as between M_9 and M_{28}, are incorrect since these are of different symmetry. The overall conclusion was that the lower wavenumber band was assignable to M_9, but only on the basis that this was the assignment put forward in the ZEKE paper[24] (note the switch in wavenumber ordering of the M_8 and M_9, not accounted for in ref. 24, discussed above); in fact, the M_9 fundamental was not seen in the DF spectrum, although a feature assigned to the $M_{12}M_{28}$ transition (b_2 symmetry) was observed. In fact, assignments were made of intense features that included those of both b_2 and a_1 symmetry, which is unusual. The 964 cm^{-1} band was assigned in ref. 14 to the b_2 symmetry band, M_{28}, although previous studies had established this at 1068 cm^{-1}.[7]

To gain more insight we compare with the DF spectra of FBz by Butler et al.[28] who also dispersed the fluorescence from equivalent levels. Looking at the DF spectrum for FBz when exciting M_9, strong bands corresponding to the M_9, M_9^2 and $M_9 M_{10}$ transitions were seen, as well as the M_{10} fundamental and many higher wavenumber features. To be consistent with the assignment of the 966 cm^{-1} band to M_9, then the DF for ClBz-h_5 should show bands at 1006 and 2012 cm^{-1}, which are not seen. Although we initially considered that there had been a misassignment of the ClBz DF spectrum in ref. 14, the wavenumbers of the observed features do appear to be consistent with the assignments offered. A possible explanation for this conundrum lies in the fact that the S_1 states of the halobenzenes undergo rapid predissociation (leading to breaking of the carbon-halogen bond) via intersystem crossing to a repulsive region of a triplet nσ* state[42] and this becomes more marked as the atomic number of the halogen atom increases, owing to the crossing point becoming increasingly closer to the minimum along the carbon-halogen bond. We note that Deguchi et al.[43] have measured the lifetime of the origin of the S_1 state using a picosecond laser as 520 ps; furthermore, we note that Liu et al.[44] have undertaken an ultrafast dynamics study of ClBz, exciting to the S_1

state at a wavenumber of ~ 37495 cm^{-1} using a femtosecond laser which was centred roughly on M_{29}, but with a width of ~ 550 cm^{-1}. Here, the lifetime of these levels was measured as having two components of 152±3 fs and 749±21 ps. In these latter two experiments,[43,44] the population of the S_1 state was monitored via photoionization. It can be expected for the lifetimes to shorten at higher wavenumbers; as such, reliable DF spectra will be difficult to obtain, with population being rapidly lost and/or transferred to different levels. Lifetimes are also expected to shorten with increasing mass of the halogen because of intersystem crossing (ISC) and predissociation noted above; indeed, no LIF or REMPI spectrum has ever been reported for iodobenzene, attributed to this short lifetime,[11,45] caused by internal conversion (IC) to a repulsive region of a singlet nσ* state (in contrast to ISC for the other monohalobenzenes); [42] however, it was possible for Kwon et al.[25] to record a one-colour MATI spectrum of iodobenzene, since here the predissociating S_1 state is bypassed.

We also note that in the laser-induced fluorescence spectrum of Imhof and Kleinermanns,[14] the intensity of the M_8 and M_9 and higher-wavenumber bands are apparently much weaker than they are in the present REMPI spectrum, suggesting the short lifetime of the state is a reasonable explanation for the above observations. The reason this lifetime effect is not evident in our spectra is that REMPI spectroscopy relies on ionization, which is extremely rapid and hence is far less susceptible to such effects;[45] in contrast, fluorescence spectroscopies require the excited state to exist long enough to emit a photon. This being the case, then the emission from these energy levels is likely not purely due to the initial excited vibrational level in the S_1 state, but rather to what remains of this, plus any emitting levels to which the population has transferred. It is worth noting that Bass and Sponer[15] commented that they did not detect any phosphorescence in their experiments, consistent with predissociation being the likely mechanism for the loss of signal.

Similar comments apply to the band at 932.2 cm^{-1}, which is assigned as M_8 in the present work, and observed in the REMPI-PES[12,21] and ZEKE[24] studies. It is less straightforward to compare the DF spectrum from this band with that of FBz, as it has been shown that in FBz the M_8 mode is in Fermi resonance with the $M_{15}M_{20}$ combination band;[28] however, the structure seen via the Fermi resonance component that has the major contribution from the M_8 vibration, displays the fundamental and overtone of this vibration. We also note that the shift in the S_0 wavenumber between FBz and ClBz is small for these vibrations, and so

similar structure involving these modes is expected. Thus, again we think this level is affected by population loss/transfer in ClBz.

(c) $M_{10}M_{11}/M_6$

We now turn to the DF spectra[14] from the two features at 1043.0 and 1066.0 cm^{-1} (reported at 1045 and 1068 cm^{-1} in that work). It transpires that these are also not straightforward to understand in terms of the expected activity of the excited S_1 vibrational state. As above, we note that a large number of intense features are assigned, which are associated with vibrations of both a_1 and b_2 symmetry. We additionally note that, except for the $M_{10}M_{11}$ band, which is seen via the 1066.0 cm^{-1} level, the assignment of the bands is not consistent with the ZEKE spectrum, nor expectations based on previous work on FBz[28] and toluene.[34] As with the DF spectra at 932.2 and 964.8 cm^{-1} we are of the opinion that these higher levels are affected by state crossings and as a consequence the DF spectrum is not (solely) representative of the initially excited level.

4. CONCLUDING REMARKS

In this work we have presented electronic spectra of the $S_1 \leftarrow S_0$ transition of four isotopologues of ClBz up to ~3000 cm^{-1}, using REMPI spectroscopy. Detailed assignments of the first ~1100 cm^{-1} of the spectra have been presented and fairly comprehensive indicative assignments given up to ~2500 cm^{-1}. For higher wavenumber regions, assignments of selected features were put forward for features that comprise clusters of vibrations. The assignments for ^{35}ClBz-h_5 have been linked to those of FBz and toluene, revealed by the consistent labelling of the vibrational modes. The shifts in wavenumber upon deuteration indicated by quantum chemical calculations have then allowed the assignments of the vibrations of ^{35}ClBz-d_5. Comparisons of the shifts previously seen in FBz upon deuteration have helped to confirm these. In both cases, $^{35/37}$Cl shifts have proven useful in deciding between possible assignments for many features; particularly notable is the shift for the M_{11} mode. A summary of the fundamental wavenumbers for all four isotoologues is included in Table S3 of the Supplementary Material.[39]

With regard to the DF studies, we find that the assignments offered in ref. 14 for vibrations with wavenumbers in the range 900-1200 cm^{-1} are not consistent with those discussed here. On the other hand, the lower wavenumber region is consistent with the present work as well as to similar DF spectra for FBz from Butler et al.[28] We rationalize the discrepant higher

wavenumber assignments by noting that ClBz undergoes very rapid predissociation and it is expected that the rate for this will increase with energy above the zero-point level. Hence, while ionization techniques, such as REMPI, ZEKE and MATI are fast and so compete with the predissociation process, this is not the case for fluorescence techniques and consequently emission is not solely from the $S_1 \rightarrow S_0$ process; direct absorption techniques bypass the predissociating state, of course. We have also noted that there are inconsistencies in the assignments of some features and the intensities observed in ZEKE spectra[24] recorded via these resonant levels – this should be investigated further.

It is clear from the assignments and discussion above, that there are a number of possible Fermi resonances in these isotopologues, in addition to the well-known one at ~520 cm^{-1} for ^{35}ClBz-h_5. Consequently, in future work it would be interesting to characterize these in more detail as was done for the 520 cm^{-1} FR by REMPI-PES,[21] MATI,[26] ZEKE[24] and DF[14] spectroscopies; other possible techniques are picosecond time-resolved photoelectron spectroscopy (see, for example, ref. 34, and references cited therein) and two-dimensional LIF.[46] These latter techniques would be especially useful for the complex Fermi resonances where there are three or more contributing ZOSs. The identification of the coupled vibrational modes in molecules allows an understanding of energy flow through the vibrational modes. This is particularly pertinent for excited states as it gives insight as to how various photophysical processes proceed, as curve crossings and conical intersections are accessed along particular vibrational coordinates at particular energies.

ACKNOWLDGEMENTS

We are grateful to the EPSRC for funding (grants EP/I012303/1 and L021366/1) and for a studentship to J.P.H. The EPSRC and the University of Nottingham are thanked for studentships to A.A. and W.D.T. We are grateful to the NSCCS for the provision of computer time under the auspices of the EPSRC, and to the High Performance Computer resource at the University of Nottingham.

Figure Captions:

Figure 1. Complete 0–3000 cm^{-1} spectral range scan of the $S_1 \leftarrow S_0$ (1+1) REMPI spectra of ClBz-h_5 (top trace, upright) and ClBz-d_5 (bottom trace, inverted) showing selected assignments – see text for further discussion. (The final vibrational level is given with all transitions emanating from the ground state zero point vibrational level; M_x^n represents a transition to n quanta of the M_x vibration.)

Figure 2. Generalized Duschinsky matrix between vibrational modes of the S_0 states of FBz-h_5 and ClBz-h_5. Shadings indicate the mixing coefficient values, with black = 1.00 while white = 0.00, with the level of the grey shading indicating intermediate values. The numbers are the i values for each M_i mode. See text for details.

Figure 3. Generalized Duschinsky matrix between the vibrational modes of the S_0 states of ClBz-h_5 and ClBz-d_5. Shadings indicate the mixing coefficient values, with black = 1.00 while white = 0.00, with the level of the grey shading indicating intermediate values. The numbers are the i values for each M_i or M_i^d mode. See text for details.

Figure 4. Generalized Duschinsky matrices between the vibrational modes of the S_1 and S_0 states for: (a) ClBz-h_5 and (b) ClBz-d_5. Shadings indicate the mixing coefficient values, with black = 1.00 while white = 0.00, with the level of the grey shading indicating intermediate values. The numbers are the i values for each M_i or M_i^d mode. See text for details.

Figure 5. Expanded views of the low wavenumber regions (0–530 cm^{-1}) of the $S_1 \leftarrow S_0$ (1+1) REMPI spectra of ClBz-h_5 (top trace, upright) and ClBz-d_5 (bottom trace, inverted). Some weak bands, marked with "Ar" are attributed to the ClBz-Ar complex. (The final vibrational level is given with all transitions emanating from the ground state zero point vibrational level; M_x^n represents a transition to n quanta of the M_x vibration.) The dashed line show a very weak feature whose assignment is very tentative.

Figure 6. Expanded views of the medium wavenumber regions (530–1120 cm^{-1}) of the $S_1 \leftarrow S_0$ (1+1) REMPI spectra of ClBz-h_5 (top trace, upright) and ClBz-d_5 (bottom trace, inverted). As indicated, expanded views are shown of three sections of the ClBz-d_5 spectrum. Assignments are discussed in the text and summarized in Tables 4 and 5; suggested assignments for some of the weaker features are also given in these tables. Some weak bands, marked with "Ar" are attributed to the ClBz-Ar complex. (The final vibrational level is given

with all transitions emanating from the ground state zero point vibrational level; M_x^n represents a transition to n quanta of the M_x vibration.)

Figure 7. Expanded views of regions γ and γ^d of the spectra in Figure 6 for ClBz-h_5 (upright, upper trace) and ClBz-d_5 (inverted, lower trace). The solid lines are the traces for the ^{35}Cl isotopologues, while the dashed lines are those for the ^{37}Cl isotopologues. See text. (Note that it was not possible to exclude completely the ^{35}ClBz isotopologue mass signal from the ^{37}ClBz mass gate, and so some contributions of the former may be contributing to the spectrum of the latter in the "unshifted" positions.) (The final vibrational level is given with all transitions emanating from the ground state zero point vibrational level; M_x^n represents a transition to n quanta of the M_x vibration.)

Figure 8. Generalized Duschinsky matrices between the vibrational modes of: (a) the S_0 and D_0^+ states for ClBz-h_5 and (b) the S_1 and the D_0^+ states for ClBz-h_5. Shadings indicate the normalized coefficient values, with black = 1.00 while white = 0.00, with the level of the grey shading indicating intermediate values. The numbers are the i values for each M_i/M_i^+ mode. See text for details.

Figure 1.

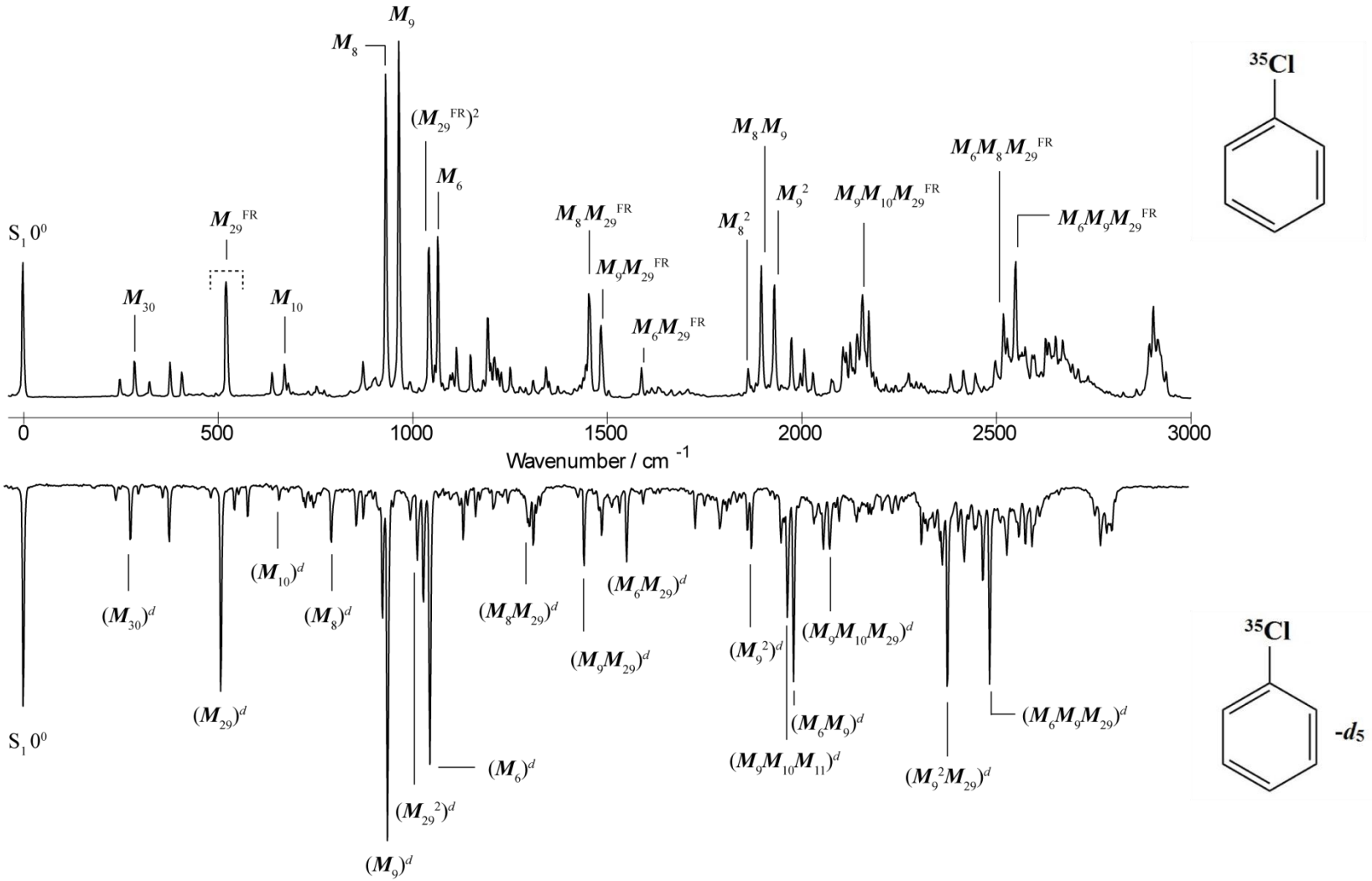
S1 0⁰
M30
M29FR
M10
M8
M9
(M29FR)2
M6
M8M29FR
M9M29FR
M6M29FR
M8M9
M8²
M9²
M9M10M29FR
M6M8M29FR
M6M9M29FR
0
500
1000
1500
2000
2500
3000
Wavenumber / cm -1
(M30)d
(M29)d
(M10)d
(M8)d
(M9)d
(M29²)d
(M6)d
(M8M29)d
(M6M29)d
(M9M29)d
(M9²)d
(M9M10M29)d
(M6M9)d
(M9M10M11)d
(M9²M29)d
(M6M9M29)d
35Cl
35Cl
-d5

Figure 2.

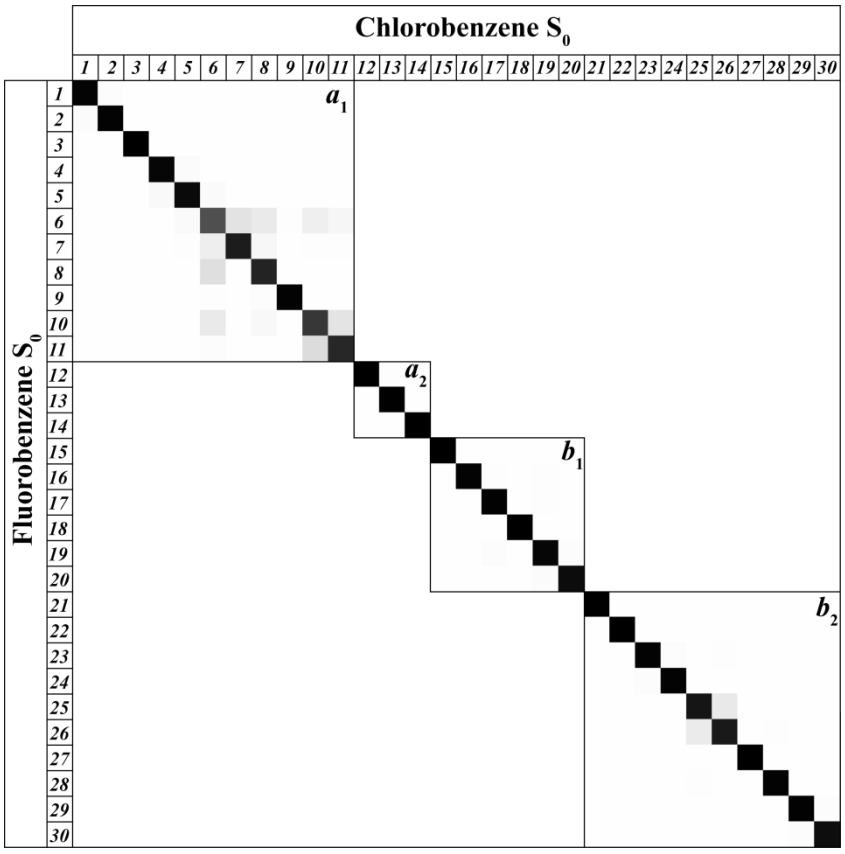

Figure 3.

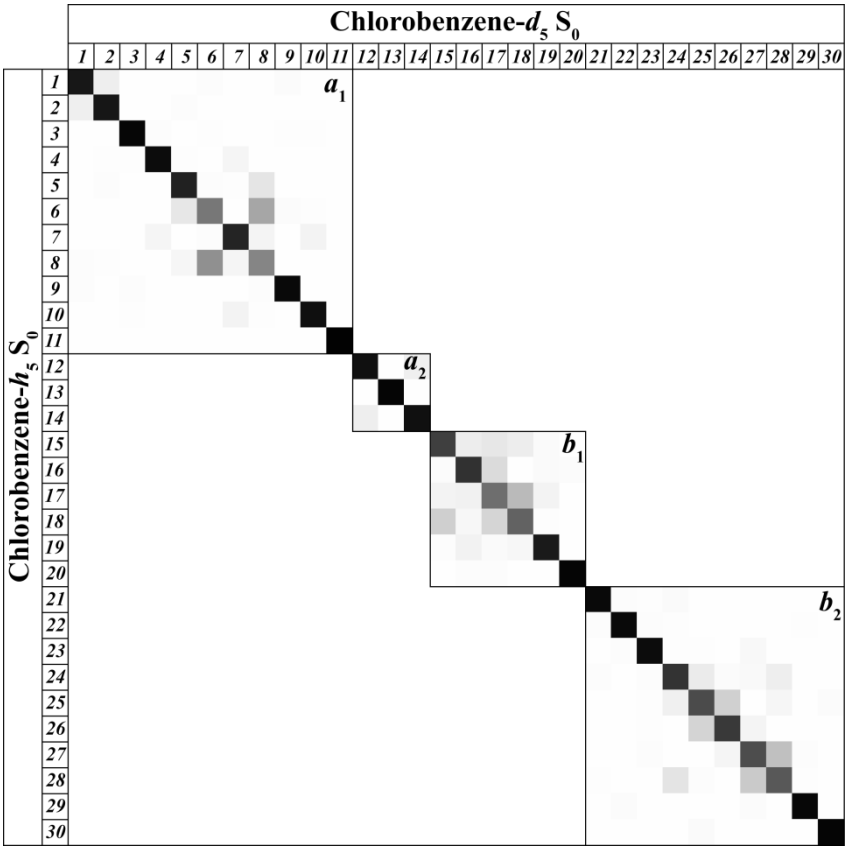

Figure 4.

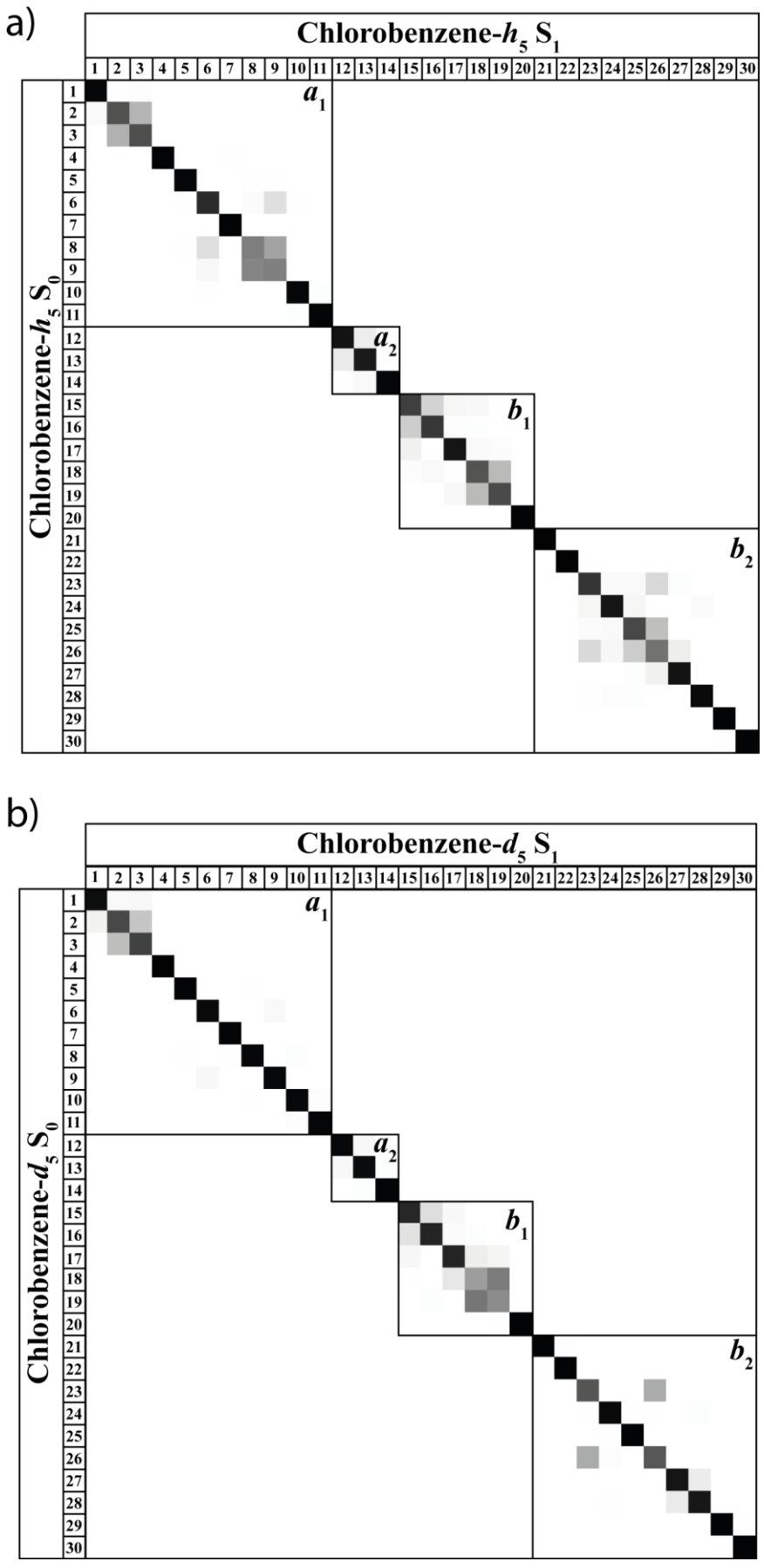
a)
Chlorobenzene-h_5 S_1
Chlorobenzene-h_5 S_0
a_1
a_2
b_1
b_2
b)
Chlorobenzene-d_5 S_1
Chlorobenzene-d_5 S_0
a_1
a_2
b_1
b_2

Figure 5.

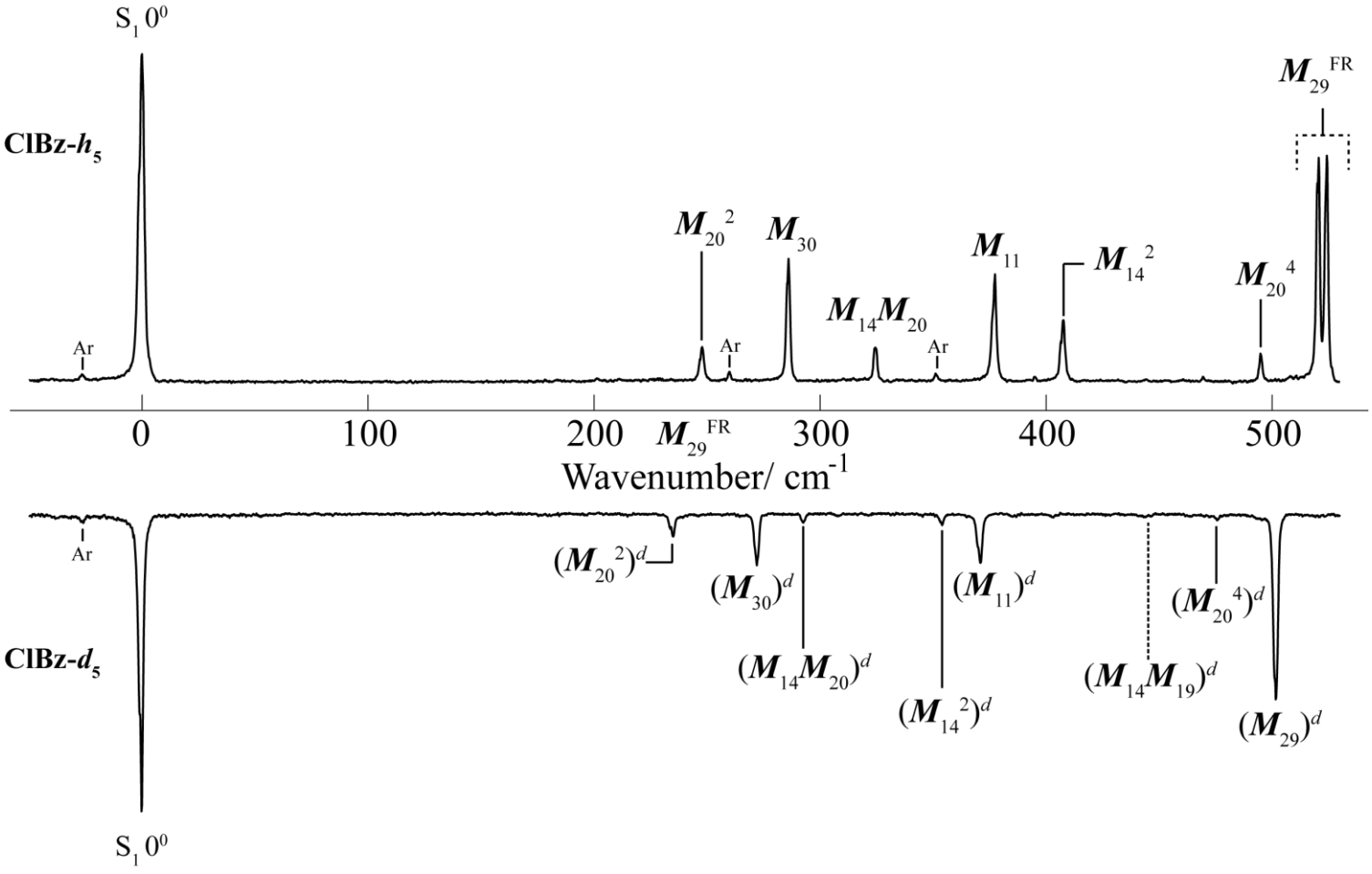
S1 0⁰
ClBz-h5
Ar
M20 2
M30
M14M20
Ar
M11
M14 2
M20 4
M29 FR
Ar
0
100
200
M29 FR
300
400
500
Wavenumber/ cm-1
Ar
ClBz-d5
S1 0⁰
(M20 2)d
(M30)d
(M14M20)d
(M14 2)d
(M11)d
(M14M19)d
(M20 4)d
(M29)d

Figure 6.

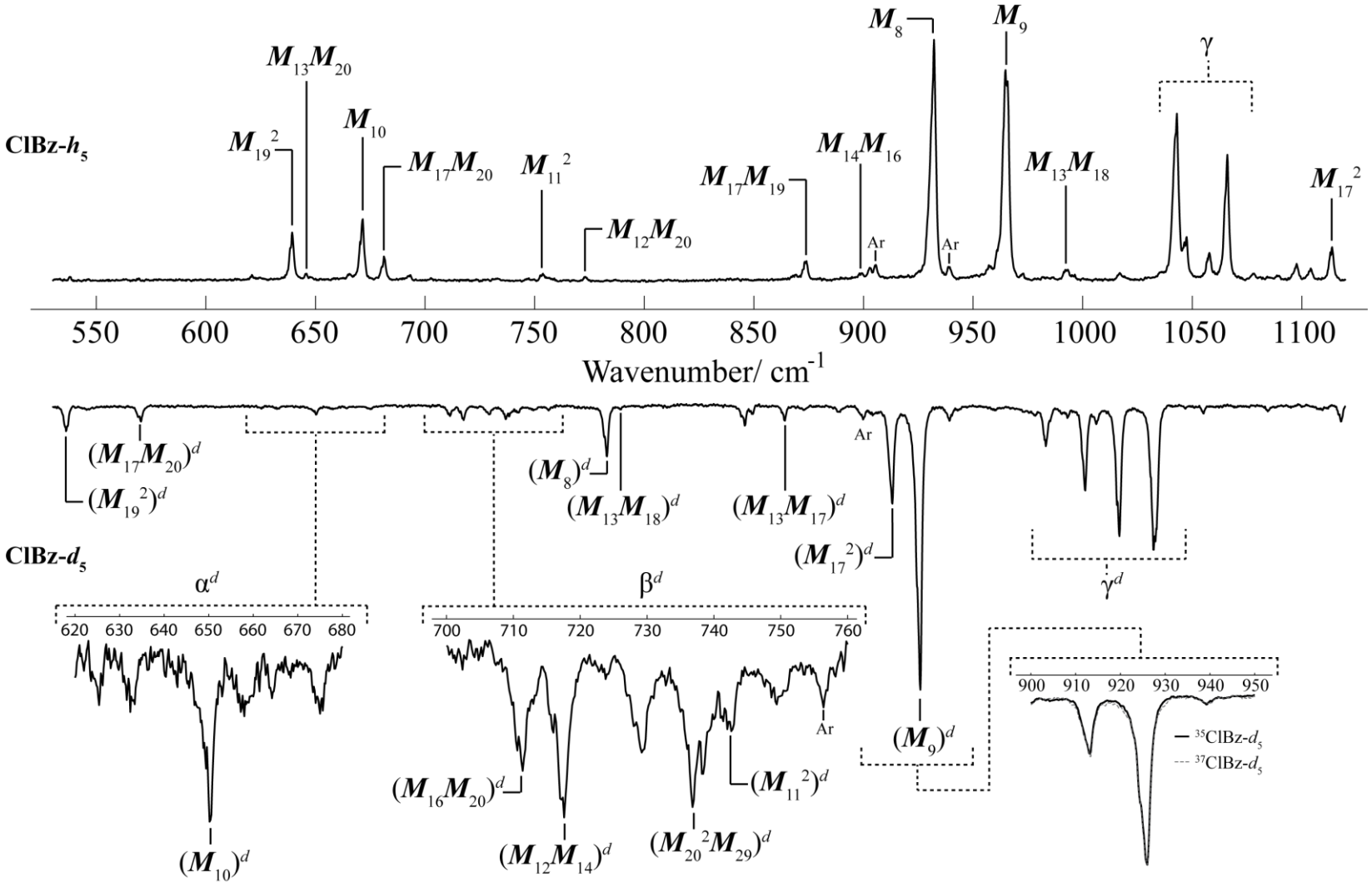
ClBz-h_5
M_{19}^2
$M_{13}M_{20}$
M_{10}
$M_{17}M_{20}$
M_{11}^2
$M_{12}M_{20}$
$M_{17}M_{19}$
$M_{14}M_{16}$
Ar
M_8
Ar
M_9
$M_{13}M_{18}$
γ
M_{17}^2
550 600 650 700 750 800 850 900 950 1000 1050 1100
Wavenumber/ cm^{-1}
$(M_{17}M_{20})^d$
$(M_{19}^2)^d$
$(M_8)^d$
$(M_{13}M_{18})^d$
$(M_{13}M_{17})^d$
Ar
$(M_{17}^2)^d$
γ^d
ClBz-d_5
α^d
620 630 640 650 660 670 680
$(M_{10})^d$
β^d
700 710 720 730 740 750 760
$(M_{16}M_{20})^d$
$(M_{12}M_{14})^d$
$(M_{20}^2M_{29})^d$
$(M_{11}^2)^d$
Ar
$(M_9)^d$
900 910 920 930 940 950
^{35}ClBz-d_5
^{37}ClBz-d_5

Figure 7.

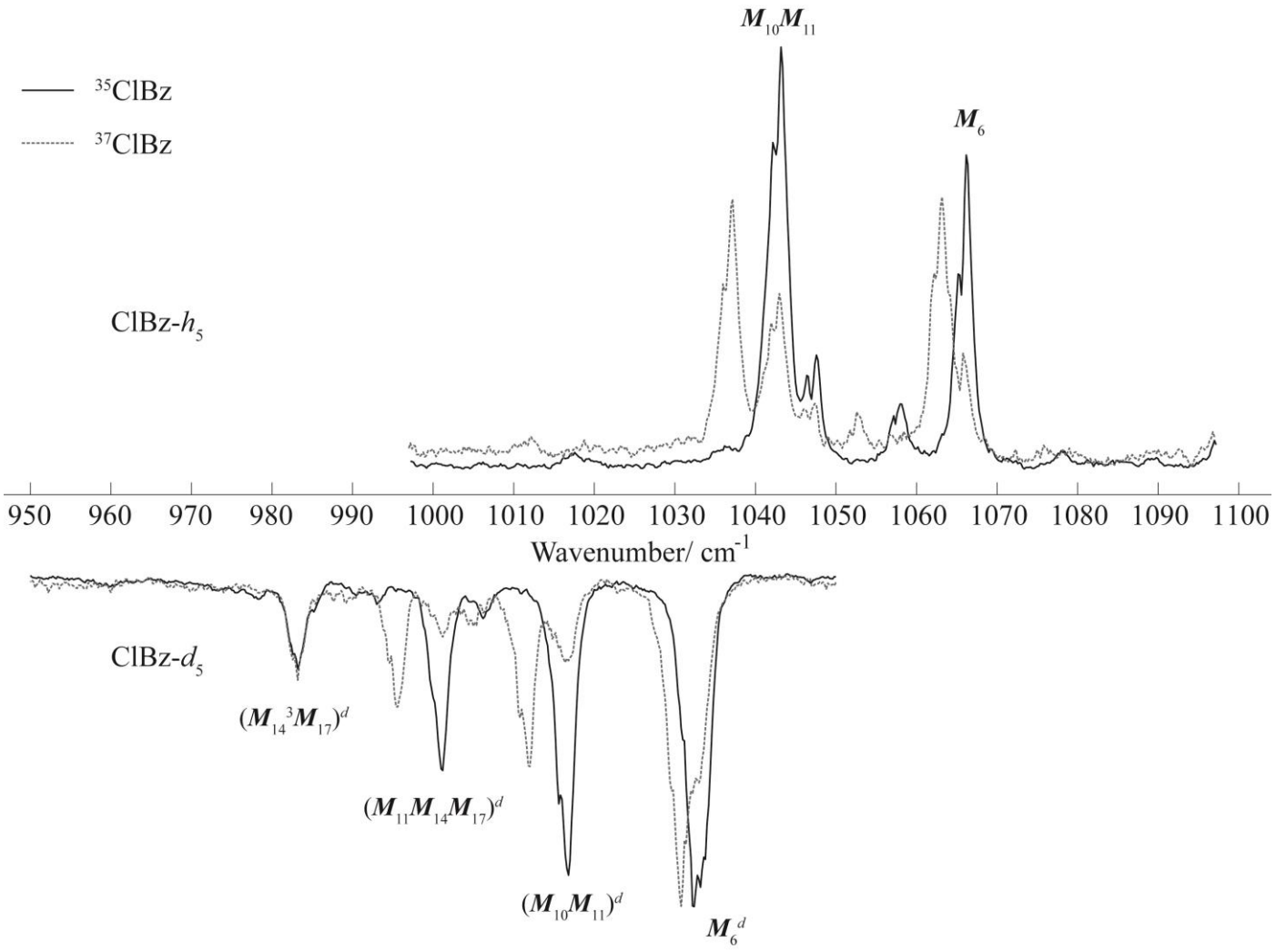
$M_{10}M_{11}$
M_6
^{35}ClBz
^{37}ClBz
ClBz-h_5
950 960 970 980 990 1000 1010 1020 1030 1040 1050 1060 1070 1080 1090 1100
Wavenumber/ cm^{-1}
ClBz-d_5
$(M_{14}{}^3M_{17})^d$
$(M_{11}M_{14}M_{17})^d$
$(M_{10}M_{11})^d$
$M_6{}^d$

Figure 8.

a)

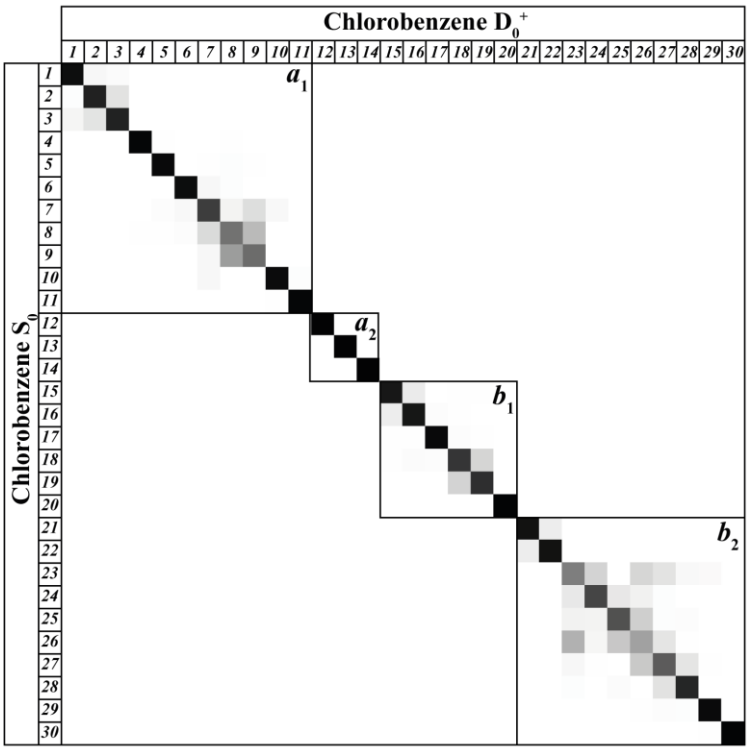
Chlorobenzene D_0^+
1 2 3 4 5 6 7 8 9 10 11 12 13 14 15 16 17 18 19 20 21 22 23 24 25 26 27 28 29 30
Chlorobenzene S_0
1 2 3 4 5 6 7 8 9 10 11 12 13 14 15 16 17 18 19 20 21 22 23 24 25 26 27 28 29 30
a_1
a_2
b_1
b_2

b)

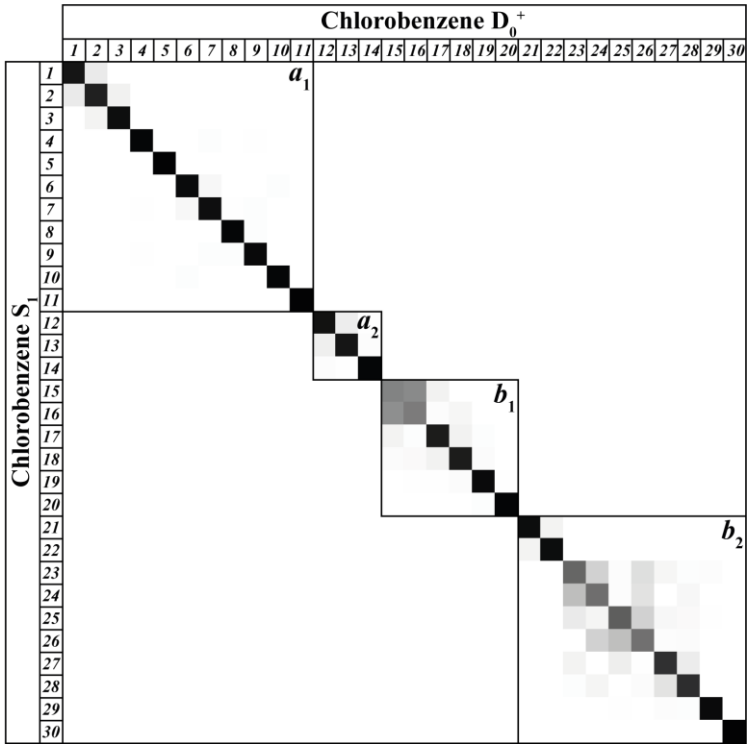
Chlorobenzene D_0^+
1 2 3 4 5 6 7 8 9 10 11 12 13 14 15 16 17 18 19 20 21 22 23 24 25 26 27 28 29 30
Chlorobenzene S_1
1 2 3 4 5 6 7 8 9 10 11 12 13 14 15 16 17 18 19 20 21 22 23 24 25 26 27 28 29 30
a_1
a_2
b_1
b_2

Table 1. Labels for ClBz-h_5 S_0 state vibrations.

Mode Label	Wilson			Mixed	
	Varsányi[a]	IR/Raman[b]	IK[c]	Benzene[d]	FBz[e]
			a_1		
$\boldsymbol{M_1}$	20a	2	2	**2**,7a,13	$\boldsymbol{M}_1$
$\boldsymbol{M_2}$	2	20a	20a	**20a**,7a,2,(13)	$\boldsymbol{M}_2$
$\boldsymbol{M_3}$	13	13	7a	**13**,7a	$\boldsymbol{M}_3$
$\boldsymbol{M_4}$	8a	8a	8a	**9a**	$\boldsymbol{M}_4$
$\boldsymbol{M_5}$	19a	19a	19a	**18a**	$\boldsymbol{M}_5$
$\boldsymbol{M_6}$	1	7a	$\nu_{C\text{-}Cl}$	**19a**, 1, (12, 20a)	$\boldsymbol{M}_6$ (M_8, M_{10}, M_7)
$\boldsymbol{M_7}$	9a	9a	9a	**8a**	$\boldsymbol{M}_7$ (M_6)
$\boldsymbol{M_8}$	18a	18a	18a	19a,1,12	$\boldsymbol{M}_8$ (M_6)
$\boldsymbol{M_9}$	12	1	12	**12,**1	$\boldsymbol{M}_9$
$\boldsymbol{M_{10}}$	6a	12	1	**6a** (20a)	$\boldsymbol{M}_{10}$ (M_{11})
$\boldsymbol{M_{11}}$	7a	6a	6a	6a, 7a, 20a (13)	$\boldsymbol{M}_{11}$ (M_{10})
			a_2		
$\boldsymbol{M_{12}}$	17a	17a	17a	**17a**	$\boldsymbol{M}_{12}$
$\boldsymbol{M_{13}}$	10a	10a	10a	**10a**	$\boldsymbol{M}_{13}$
$\boldsymbol{M_{14}}$	16a	16a	16a	**16a**	$\boldsymbol{M}_{14}$
			b_1		
$\boldsymbol{M_{15}}$	5	5	5	**5**, 17b	$\boldsymbol{M}_{15}$
$\boldsymbol{M_{16}}$	17b	17b	17b	17b, 10b,(5, 11)	$\boldsymbol{M}_{16}$
$\boldsymbol{M_{17}}$	11	10b	11	11, 10b,(4, 17b)	$\boldsymbol{M}_{17}$
$\boldsymbol{M_{18}}$	4	4	4	**4** (11)	$\boldsymbol{M}_{18}$
$\boldsymbol{M_{19}}$	16b	16b	16b	**16b**, (11, 10b)	$\boldsymbol{M}_{19}$
$\boldsymbol{M_{20}}$	10b	11	10b	(16b, 10b, 17b, 11)	$\boldsymbol{M}_{20}$
			b_2		
$\boldsymbol{M_{21}}$	20b	20b	20b	**20b**, (7b)	$\boldsymbol{M}_{21}$
$\boldsymbol{M_{22}}$	7b	7b	7b	**7b**,(20b)	$\boldsymbol{M}_{22}$
$\boldsymbol{M_{23}}$	8b	8b	8b	**9b**	$\boldsymbol{M}_{23}$
$\boldsymbol{M_{24}}$	19b	19b	19b	**18b**, (3)	$\boldsymbol{M}_{24}$
$\boldsymbol{M_{25}}$	14	3	3	**3**, 15, (8b)	$\boldsymbol{M}_{25}$
$\boldsymbol{M_{26}}$	3	14	14	**15**, 3, (8b)	$\boldsymbol{M}_{26}$ (M_{25})
$\boldsymbol{M_{27}}$	9b	9b	9b	**14**, 8b	$\boldsymbol{M}_{27}$
$\boldsymbol{M_{28}}$	18b	15	18b	**19b**, (8b, 14)	$\boldsymbol{M}_{28}$
$\boldsymbol{M_{29}}$	6b	6b	6b	**6b**	$\boldsymbol{M}_{29}$
$\boldsymbol{M_{30}}$	15	18b	15	(8b, 19b, 14, 18b, 3, 6b)	$\boldsymbol{M}_{30}$

[a] Ref. 20

[b] As summarized in ref. 24 from refs. 2, 7 and 8.

[c] Ref.14

[d] M_i modes expressed in terms of benzene Wilson modes using a generalized Duschinsky matrix approach using B3LYP/aug-cc-pTVZ calculations. These are similar to the values reported in ref. 9, where the mixings were obtained using the B3LYP/aug-cc-pDVZ method.

Values outside parentheses have mixing coefficients > 0.2 and are termed major contributions, with bolded values being dominant contributions (mixing coefficients > 0.5). Those inside parentheses are minor contributions, and have values between 0.05 and 0.2. If there is more than one contribution of each type, these are given in numerical order. Vibrations with a mixing coefficient < 0.05 are ignored.

[e] M_i modes of ClBz expressed in terms of those FBz. Values outside parentheses have mixing coefficients > 0.2 and are termed major contributions, with bolded values being dominant contributions (mixing coefficients > 0.5). Those inside parentheses are minor contributions, and have values between 0.05 and 0.2. If there is more than one contribution of each type, these are given in numerical order. Vibrations with a mixing coefficient < 0.05 are ignored.

Table 2. Assignments, calculated and experimental vibrational wavenumbers (cm^{-1}) for the S_0 state of ^{35}ClBz-h_5 and ^{35}ClBz-d_5.

	ClBz-h_5							**ClBz-d_5**		
Mode label	Calculated					Experimental		**Mode Label**	Calculated	Experimental
	This work[a]	B3LYP[b]	B3LYP[c]	MP2[d]	CAS(8,7)[e]	IR/Raman[f]	DF[g]		This work[a]	IR/Raman[h]
a_1										
M_1	3109	3213	3204	3240	3383	3082		M_1^d	2303	2295
M_2	3097	3199	3191	3230	3368	3054		M_2^d	2291	2288
M_3	3076	3178	3169	3209	3344	3031		M_3^d	2268	-
M_4	1571	1622	1628	1632	1725	1586		M_4^d	1535	1563
M_5	1466	1492	1509	1508	1622	1483		M_5^d	1333	1346
M_6	1065	1097	1098	1129	1177	1092	1097	M_6^d	1015	1038
M_7	1161	1187	1197	1199	1271	1153		M_7^d	852	865
M_8	1013	1040	1098	1044	1149	1025		M_8^d	814	816
M_9	990	1009	1016	1004	1064	1003	1006	M_9^d	949	959
M_{10}	687	707	754	718	767	706	710	M_{10}^d	656	667
M_{11}	401	414	417	422	443	417	417	M_{11}^d	394	412
a_2										
M_{12}	962	976	978	904	997	961		M_{12}^d	783	760
M_{13}	825	834	841	816	856	832		M_{13}^d	642	680
M_{14}	404	417	414	394	433	403	404.5[j]	M_{14}^d	351	367
b_1										
M_{15}	983	1000	1003	897	1028	981		M_{15}^d	820	-
M_{16}	903	913	917	855	933	902		M_{16}^d	747	747
M_{17}	739	751	708	718	753	741		M_{17}^d	612	618
M_{18}	681	704	703	365	726	685		M_{18}^d	541	542
M_{19}	467	484	480	441	513	467		M_{19}^d	408	420
M_{20}	183	188	187	183	204	198[i]	185.5[j]	M_{20}^d	172	182
b_2										
M_{21}	3107	3211	3202	3237	3380	3096		M_{21}^d	2299	-
M_{22}	3084	3187	3178	3218	3355	3067		M_{22}^d	2278	-
M_{23}	1576	1626	1624	1631	1718	1598		M_{23}^d	1541	1543
M_{24}	1435	1462	1478	1445	1577	1448		M_{24}^d	1309	1260
M_{25}	1306	1344	1343	1474	1443	1326		M_{25}^d	1018	1022
M_{26}	1277	1314	1183	1181	1191	1271		M_{26}^d	1274	1322
M_{27}	1146	1172	1318	1326	1311	-		M_{27}^d	831	842
M_{28}	1064	1092	1043	1098	1101	1068	1063	M_{28}^d	807	800
M_{29}	609	623	628	617	661	615	616	M_{29}^d	584	591
M_{30}	286	296	298	296	317	295	294	M_{30}^d	271	282

[a] B3LYP/aug-cc-pVTZ values, scaled by 0.97.
[b] B3LYP/aug-cc-pVDZ, unscaled.[9]
[c] B3LYP/6-311G(d,p), unscaled.[14]
[d] MP2/6-311G(d,p), unscaled.[14]
[e] CAS(8,7)/6-31++G(d,p), unscaled.[14]
[f] As summarized in ref. 24 from refs. 2, 7 and 8.
[g] Dispersed fluorescence results from ref. 14 – see text for discussion.
[h] Originally from ref. 19, but tabulated and relabelled in ref. 20.
[i] denotes a Raman value in liquid sample from ref. 7
[j] M_{14} and M_{20} fundamentals have been obtained from overtones reported in ref. 14

Table 3. Assignments, calculated and experimental vibrational wavenumbers (cm^{-1}) for the S_1 state of ^{35}ClBz-h_5 and ^{35}ClBz-d_5

Mode Label	^{35}ClBz-h_5						Mode Label	^{35}ClBz-d_5	
	Calculated		Experimental					Calculated	Experimental
	This work[a]	CAS(8,7)[b]	This work	Wright et al.[c]	Bist et al.[d]	Asselin et al.[e]		This work[a]	This work
					a_1				
M_1	3135	3404		-	3158.2		M_1^d	2320	
M_2	3116	3386		-	3118.7		M_2^d	2301	
M_3	3087	3365		-	3083.4		M_3^d	2276	
M_4	1478	1659		-	1564.3		M_4^d	1434	
M_5	1402	1540		-	1489.0		M_5^d	1238	
M_6	1034	1131	1066.0[h]	1066	1065.1	1064.2	M_6^d	1003	1032.4
M_7	1129	1241		-	980.6		M_7^d	833	
M_8	946	1028	932.2	932	965.7	929.2	M_8^d	785	783.2
M_9	969	970	964.8	965	931.3	964.2	M_9^d	918	926.2
M_{10}	673	709	671.6	-	671.3		M_{10}^d	641	650.4
M_{11}	374	412	377.4	-	378.2	378.2	M_{11}^d	367	371.2
					a_2				
M_{12}	642	659	*649.3*[g]	-			M_{12}^d	532	*540.7*[g]
M_{13}	523	574	*522.1*[g]	-			M_{13}^d	412	*407.0*[g]
M_{14}	119	284	203.8[g]	-	203.07[f]		M_{14}^d	100	177.1[g]
					b_1				
M_{15}	825	719		-			M_{15}^d	704	
M_{16}	694	640	*694.4*[g]	-			M_{16}^d	594	*594.1*[g]
M_{17}	580	551	557.3[g]	-			M_{17}^d	455	456.7[g]
M_{18}	474	474	*471.1*[g]	-			M_{18}^d	383	382.6[g]
M_{19}	340	272	319.7[g]	-	320.49[f]		M_{19}^d	291	268.2[g]
M_{20}	136	118	123.9[g]	-			M_{20}^d	129	117.5[g]
					b_2				
M_{21}	3129.9	3399		-	3076.0		M_{21}^d	2310	
M_{22}	3108.8	3376		-	3056.0		M_{22}^d	2287	
M_{23}	1446.0	1848		-[h]	1584.4		M_{23}^d	1376	
M_{24}	1375.5	1503		-[h]	1483.2		M_{24}^d	1205	
M_{25}	1263.9	1401		1564[i]	1210.1		M_{25}^d	999	
M_{26}	1393.4	1649		-	1194.3		M_{26}^d	1413	
M_{27}	1133.2	1253		-	1149.4		M_{27}^d	819	
M_{28}	977.6	1015		-	1089.7		M_{28}^d	775	
M_{29}	512.1	587	520.6[j]	521.3	521.0	521.8	M_{29}^d	493	501.8
M_{30}	286.0	307	286.0	287.8	287.3	288.2	M_{30}^d	271	272.2

[a] TDDFT, B3LYP/aug-cc-pVTZ, scaled by 0.97.
[b] Ref. 14. CAS(8,7)/ 6-31++G(d,p)
[c] Ref. 24
[d] Ref. 6 and 8
[e] Ref. 21
[f] Derived from an overtone band from ref. 8
[g] Derived from a combination band or overtone. Italicized values are less certain.
[h] Values are given in ref. 24 for these vibrations, but these have been reassigned here to combination bands (see Table 4).
[i] Seen in two-photon REMPI experiments[10] – see text for discussion.
[j] Fermi resonance component – see text.

Table 4. A summary of the assigned vibrational features from the present work for the $S_1 \leftarrow S_0$ transition of the ^{35}ClBz-h_5. (The final vibrational level is given with all transitions emanating from the ground state zero point vibrational level; M_x^n represents a transition to n quanta of the M_x vibration.)

^{35}ClBz-h_5				
Experimental band (cm^{-1})[a]	Assignment[b]	This work B3LYP	From experimental fundamentals seen[c]	Overall symmetry
-26.6	[0^0 + Ar]	-	-	-
0.0	0^0	-	-	-
247.8	M_{20}^2	272.7	247.8[d]	a_1
259.6	[M_{30}+Ar]		-26.4 from M_{30}	
286.0	M_{30}	285.9	286.0[d]	b_2
324.4	$M_{14}M_{20}$	255.5	327.7	b_2
351.0	[M_{11}+Ar]		-26.4 from M_{11}	
377.4	M_{11}	374.5	377.4[d]	a_1
407.6	M_{14}^2	238.4	407.6[d]	a_1
494.8	M_{20}^4	545.3	495.6	a_1
520.6	M_{29}	512.1	520.6[d]	b_2
524.2	$M_{14}M_{19}$	459.4	523.5	b_2
538.0†	$M_{20}^2M_{30}$	558.7	533.8	b_2
621.0	$M_{14}M_{20}M_{30}$	541.5	613.7	a_1
	$M_{11}M_{20}^2$	647.1	625.2	a_1
639.4	M_{19}^2	680.5	639.4[d]	a_1
646.0†	$M_{13}M_{20}$	659.5	646.0[d]	b_2
665.6	$M_{11}M_{30}$	660.4	663.4	b_2
671.6	M_{10}	672.5	671.6[d]	a_1
681.2	$M_{17}M_{20}$	716.4	681.2[d]	a_1
693.4	$M_{14}^2M_{30}$	524.4	693.6	b_2
753.8	M_{11}^2	748.9	754.8	a_1
759.0	$M_{14}M_{17}$	699.2	761.1	b_2
773.2†	$M_{20}^2M_{29}$	784.8	768.4	b_2
	$M_{14}M_{19}M_{20}^2$	732.1	771.3	b_2
	$\boldsymbol{M_{12}M_{20}}$	778.3	773.2[d]	b_2
874.0	$M_{17}M_{19}$	920.3	877.0	a_1
898.2†	$M_{14}M_{16}$	813.2	898.2[d]	b_2
902.8	-			
905.6	[M_8+Ar]		-26.6 from M_8	
927.2	$M_{14}^2M_{29}$	750.5	928.2	b_2
	$M_{14}^3M_{19}$	697.8	931.1	b_2
	$M_{19}^2M_{30}$	966.4	925.4	b_2
	$M_{13}M_{20}M_{30}$	945.5	932.0	a_1
932.2	M_8	945.8	932.2[d]	a_1
938.6	[M_9+Ar]		- 26.2 from M_9	
957.2	$\boldsymbol{M_{10}M_{30}}$	958.5	957.6	b_2
	$M_{14}M_{18}M_{30}$	879.7	961.0	a_1
964.8	M_9	968.7	964.8[d]	a_1
973.0	M_{28}	977.6	973.0[d]	b_2
	$M_{17}M_{20}M_{30}$	1002.4	967.2	b_2
	$M_{12}M_{19}$	982.2	969.0	b_2
993.2†	$M_{13}M_{18}$	997.7	993.2[d]	b_2
1017.0	$\boldsymbol{M_{11}M_{19}^2}$	1054.9	1016.8	a_1
	$M_{11}M_{13}M_{20}$	1034.0	1023.4	b_2
1043.0	$M_{17}M_{18}$	1054.5	1028.4	a_1
	$M_{18}M_{19}M_{20}^2$	1087.4	1038.6	a_1
	$M_{11}^2M_{30}$	1034.9	1040.8	b_2
	$\boldsymbol{M_{29}^2}$	1024.2	1041.2	a_1

	M_{13}^2	1046.4	1044.2	a_1
	$\boldsymbol{M_{14}M_{19}M_{29}}$	971.5	1044.1	a_1
	$\boldsymbol{M_{10}M_{11}}$	1047.0	1049.0	a_1
1047.4	$M_{14}^2M_{19}^2$	918.8	1047.0	a_1
	$M_{14}M_{17}M_{30}$	985.2	1047.1	a_1
1057.8	$M_{11}M_{14}M_{18}$	968.1	1052.3	b_2
	$M_{13}M_{14}^2M_{20}$	897.9	1053.6	b_2
	$M_{20}^2M_{29}M_{30}$	1070.8	1054.4	a_1
	$\boldsymbol{M_{11}M_{17}M_{20}}$	1090.8	1058.6	a_1
	$M_{12}M_{20}M_{30}$	1064.3	1059.2	a_1
1066.0	M_6	1034.3	1066.0[d]	a_1
1078.2	$M_{13}M_{17}$	1103.2	1079.4	b_2
	$M_{10}M_{14}^2$	910.9	1079.2	a_1
1113.8	M_{17}^2	1160.1	1114.6[d]	a_1
1191.8	$M_{10}M_{29}$	1184.6	1192.2	b_2
1194.8	$M_{10}M_{14}M_{19}$	1131.9	1195.1	b_2
1220.0	M_8M_{30}	1231.8	1218.2	b_2
1252.4	M_9M_{30}	1254.7	1250.8	b_2
1453.4	M_8M_{29}	1457.9	1452.8	b_2
1457.2	$M_8M_{14}M_{19}$	1405.2	1455.7	b_2
1485.0	M_9M_{29}	1480.8	1485.4	b_2
1488.2	$M_9M_{14}M_{19}$	1428.2	1488.3	b_2
1587	M_6M_{29}	1546.4	1586.6	b_2
1591	$M_6M_{14}M_{19}$	1493.8	1589.5	b_2
1865	M_8^2	1891.6	1864.4	a_1
1898	M_8M_9	1914.5	1897.0	a_1
1931	M_9^2	1937.5	1929.6	a_1
1976	$M_8M_{10}M_{11}$	1992.8	1981.2	a_1
1999	M_6M_8	1980.1	1998.2	a_1
2009	$M_9M_{10}M_{11}$	2015.7	2013.8	a_1
2031	M_6M_9	2003.1	2030.8	a_1
2128	$M_8M_{10}M_{29}$	2130.4	2124.4	b_2
	$M_8M_{10}M_{14}M_{19}$	2077.7	2127.3	b_2
2159	$M_9M_{10}M_{29}$	2153.4	2157.0	b_2
	$M_9M_{10}M_{14}M_{19}$	2100.7	2159.9	b_2
2386	$M_8^2M_{29}$	2403.7	2385.0	b_2
2390	$M_8^2M_{14}M_{19}$	2351.0	2387.9	b_2
2418	$M_8M_9M_{29}$	2426.6	2417.6	b_2
	$M_8M_9M_{14}M_{19}$	2373.9	2420.5	b_2
2449	$M_9^2M_{29}$	2449.6	2450.2	b_2
2455	$M_9^2M_{14}M_{19}$	2396.9	2453.1	b_2
2522	$M_6M_8M_{29}$	2492.2	2518.8	b_2
	$M_6M_8M_{14}M_{19}$	2439.5	2521.7	b_2
2551	$M_6M_9M_{29}$	2515.2	2551.4	b_2
	$M_6M_9M_{14}M_{19}$	2462.5	2554.3	b_2

[a] Features above 1500 cm^{-1} are quoted to 1 cm^{-1} only as no 0.2 cm^{-1} stepsize scans were taken of the high wavenumber region for this isotopologue.

[b] A **bold** assignment indicates a favoured choice where multiple options are possible; if multiple options are given but none is bolded, the assignment is not known definitively. A † next to an assignment indicates a tentative assignment, but where there appears to be little else to choose from or it is the best from the options available.

[c] All values are computed entirely from experimental fundamentals.

[d] An experimental fundamental is taken from this feature.

Table 5. A summary of the assigned vibrational features from the present work for the $S_1 \leftarrow S_0$ transition of the ^{35}ClBz-d_5. (The final vibrational level is given with all transitions emanating from the ground state zero point vibrational level; M_x^n represents a transition to n quanta of the M_x vibration.)

^{35}ClBz-d_5				
Experimental band (cm^{-1})	Assignment[a]	This work B3LYP	From experimental fundamentals seen[b]	Overall symmetry
-26.2	$[0^0+Ar]$	-	-	-
0	0^0	-	-	-
235.0	$(M_{20}^2)^d$	257.1	235.0[c]	a_1
272.2	$(M_{30})^d$	271.3	272.2[c]	b_2
292.8	$(M_{14}M_{20})^d$	228.8	294.6[c]	b_2
354.2	$(M_{14}^2)^d$	200.5	354.2[c]	a_1
371.2	M_{11}^d	366.7	371.2[c]	a_1
446.6	$(M_{14}M_{19})^d$	391.3	445.3	b_2
475.8	$(M_{20}^4)^d$	514.2	470.0	a_1
501.8	M_{29}^d	492.6	501.8[c]	b_2
536.4	$\mathbf{(M_{19}^2)^d}$	582.0	536.4[c]	a_1
570.6	$(M_{17}M_{20})^d$	583.6	574.2	a_1
625.6	$(M_{14}^2M_{30})^d$	471.7	626.4	b_2
633.6	$(M_{14}M_{17})^d$	555.2	633.8	b_2
650.4	M_{10}^d	640.6	650.4	a_1
675.2†	$(M_{13}M_{19})^d$	703.2	675.2[c]	b_2
693.4	-			
711.6†	$\mathbf{(M_{16}M_{20})^d}$	722.9	711.6[c]	a_1
	$(M_{14}^4)^d$	400.9	708.4	a_1
717.8†	$\mathbf{(M_{12}M_{14})^d}$	632.0	717.8[c]	a_1
	$(M_{17}M_{19})^d$	746.0	724.9	a_1
729.4	$(M_{17}M_{19})^d$	746.0	724.9	a_1
	$(M_{18}M_{20}^3)^d$	768.9	735.1	a_1
737.0	$(M_{20}^2M_{29})^d$	749.7	736.8	b_2
742.8	$(\mathbf{M_{11}^2})^d$	733.5	742.4	a_1
	$(M_{14}^2M_{19}M_{20})^d$	620.0	739.9	a_1
756.6	$\mathbf{[M_8^d+Ar]}$		- 26.6 from M_8^d	
	$(M_{11}M_{19}M_{20})^d$	786.3	756.9	a_1
779.6	M_{28}^d	775.3	-	b_2
783.2	M_8^d	785.3	783.2[c]	a_1
789.6†	$(M_{13}M_{18})^d$	795.4	789.6[c]	b_2
846.0	$\mathbf{(M_{17}M_{20}M_{30})^d}$	854.9	846.4	b_2
	$(M_{14}M_{20}M_{30}^2)^d$	771.4	839.0	b_2
	$(M_{14}^2M_{18}M_{20})^d$	712.2	854.3	a_1
849.8	$(M_{14}^2M_{29})^d$	693.0	856.0	b_2
	$(M_{14}^2M_{18}M_{20})^d$	712.2	854.3	a_1
864.4†	$\mathbf{(M_{13}M_{17})^d}$	867.2	863.7	b_2
	$(M_{16}M_{19})^d$	885.3	862.3	a_1
	$(M_{14}M_{17}M_{20}^2)^d$	812.4	868.8	b_2
889.6	$(M_{14}^2M_{19}^2)^d$	782.5	890.6	a_1
	$(M_{19}M_{20}M_{29})^d$	912.2	887.5	b_2
	$(M_{14}^2M_{30}^2)^d$	743.0	898.6	a_1
900.0	$[M_9^d+Ar]$		- 26.2 from M_9^d	
904.4	$\mathbf{(M_{14}M_{17}M_{30})^d}$	826.5	906.0	a_1
	$(M_{11}M_{19}^2)^d$	948.5	907.6	a_1

913.4	$(M_{17}^2)^d$	910.0	913.4[c]	a_1
920.2	$(M_{10}M_{30})^d$	911.9	922.6	b_2
	$(M_{12}M_{18})^d$	915.0	923.3	b_2
926.2	M_9^d	917.6	926.2[c]	a_1
939.4	$(M_{13}M_{14}^3)^d$	712.8	938.3	a_1
	$(M_{16}M_{20}^3)^d$	979.9	946.6	a_1
983.4	$(M_{16}M_{20}M_{30})^d$	994.1	983.8	b_2
	$(M_{14}M_{19}^3)^d$	973.3	981.7	b_2
	$(M_{14}^3M_{17})^d$	755.7	988.0	b_2
993.2	$(M_{14}M_{19}M_{30}^2)^d$	933.8	989.7	b_2
	$(M_{18}^2M_{20}^2)^d$	1023.6	1000.2	a_1
	$(M_{12}M_{17})^d$	986.8	997.4	b_2
	$(M_{17}M_{19}M_{30})^d$	1017.3	997.1	b_2
	$(M_{11}M_{14}^2M_{30})^d$	838.5	997.6	b_2
	M_{25}^d	999.3	-	b_2
1001.4	$\mathbf{(M_{11}M_{14}M_{17})^d}$	922.0	1005.0	b_2
	$(M_{13}M_{16})^d$	1006.4	1001.1	b_2
	$(M_{18}M_{20}M_{29})^d$	1004.4	1001.9	b_2
	$\mathbf{(M_{29}^2)^d}$	985.2	1003.6	a_1
	$(M_{10}M_{14}^2)^d$	841.0	1004.6	a_1
	$(M_{14}M_{16}M_{20}^2)^d$	951.6	1006.2	b_2
1017.0	$\mathbf{(M_{10}M_{11})^d}$	1007.3	1021.6	a_1
	$(M_8M_{20}^2)^d$	1042.5	1018.2	a_1
	$(M_{12}M_{14}^2M_{20})^d$	860.8	1012.4	b_2
	$(M_{11}M_{18}M_{19})^d$	1041.0	1022.0	a_1
1032.6	M_6^d	1002.6	1032.4[c]	a_1
1149.0	$(M_{10}M_{29})^d$	1133.2	1152.2	b_2
1281.4	$(M_8M_{29})^d$	1277.9	1285.0	b_2
1425.4	$(M_9M_{29})^d$	1410.1	1428.0	b_2
1533.6	$(M_6M_{29})^d$	1495.2	1534.2	b_2
1850.6	$(M_9^2)^d$	1835.1	1852.4	a_1
1941.2	$(M_9M_{10}M_{11})^d$	1924.9	1947.8	a_1
1956.4	$(M_6M_9)^d$	1920.1	1958.6	a_1
2047.8	$(M_6M_{10}M_{11})^d$	2009.9	2054.0	a_1
2072.4	$(M_9M_{10}M_{29})^d$	2050.7	2078.4	b_2
2348.4	$(M_9^2M_{29})^d$	2327.7	2354.2	b_2
2455.0	$(M_6M_9M_{29})^d$	2412.7	2460.4	b_2

[a] A **bold** assignment indicates a favoured choice where multiple options are possible; if multiple options are given but none is bolded, the assignment is not known definitively. An † next to an assignment indicates a tentative assignment, but where there appears to be little else to choose from or it is the best from the options available.

[b] All values computed entirely from experimental fundamentals.

[c] An experimental fundamental is taken from this feature.

Table 6. Assignments, calculated and experimental vibrational wavenumbers (cm^{-1}) for the ground state cation, D_0^+, of ^{35}ClBz-h_5 and ^{35}ClBz-d_5.

Mode Label	ClBz-h_5^+						Mode Label	ClBz-d_5^+	
	Calculated		Experimental					Calculated	
	This work [a]	Wright et al.[b]	Asselin et al.[c]	Wright et al. [d]	Lembach and Brutschy[e]	Kwon et al.[f]		This work[a]	Asselin et al.[c]
a_1									
M_1^+	3122	3052					M_1^{d+}	2317	
M_2^+	3111	3043					M_2^{d+}	2299	
M_3^+	3099	3030					M_3^{d+}	2289	
M_4^+	1589	1619				1554	M_4^{d+}	1548	
M_5^+	1422	1393		1429			M_5^{d+}	1250	
M_6^+	1084	1072	1106	1116	1115	1118	M_6^{d+}	1059	
M_7^+	1181	1174	1182	1200	1194	1193	M_7^{d+}	851	
M_8^+	960	885	981	975	971	974	M_8^{d+}	801	760
M_9^+	977	961	1016	995	992	991	M_9^{d+}	932	
M_{10}^+	700	673	728	716	714	713	M_{10}^{d+}	665	
M_{11}^+	414	401	421	422	420	419	M_{11}^{d+}	405	413
a_2									
M_{12}^+	989	1010					M_{12}^{d+}	802	
M_{13}^+	786	808					M_{13}^{d+}	611	
M_{14}^+	344	347	342	348	343		M_{14}^{d+}	300	
b_1									
M_{15}^+	1000	1015	909				M_{15}^{d+}	843	
M_{16}^+	944	960	812				M_{16}^{d+}	771	
M_{17}^+	769	771	603			771	M_{17}^{d+}	652	
M_{18}^+	589	586	558			600?[g]	M_{18}^{d+}	470	
M_{19}^+	376	396	388	394	393	[482][g]	M_{19}^{d+}	324	
M_{20}^+	144	144	165			141	M_{20}^{d+}	134	
b_2									
M_{21}^+	3120	3050					M_{21}^{d+}	2313	
M_{22}^+	3109	3038					M_{22}^{d+}	2295	
M_{23}^+	1373	1365				1593	M_{23}^{d+}	1237	
M_{24}^+	1483	1485					M_{24}^{d+}	1394	
M_{25}^+	1249	1317					M_{25}^{d+}	1021	
M_{26}^+	1345	1113					M_{26}^{d+}	1299	
M_{27}^+	1122	1035					M_{27}^{d+}	825	
M_{28}^+	1070	1220					M_{28}^{d+}	821	
M_{29}^+	523	496	526	531	526	527	M_{29}^{d+}	507	
M_{30}^+	293	294	322	311		[286][g]	M_{30}^{d+}	278	

[a] UB3LYP/aug-cc-pVTZ, scaled by 0.97.
[b] RHF/6-31G*, scaled by 0.89, ref. 24.
[c] Two-colour REMPI-PES, ref. 21. The assignment of M_8^{d+} is suggested in the present work –see text.
[d] Two-colour ZEKE spectroscopy, ref. 24. The assignment of the 1116 cm^{-1} feature was ambiguous as a band at 1147 cm^{-1} was also mentioned in the text of that work – see discussion in the present main text.
[e] Two-colour MATI spectroscopy, ref. 26.
[f] One-colour MATI spectroscopy, ref. 25.
[g] The value marked with a "?" was uncertain in ref. 25; values in square brackets are deemed unreliable by ourselves by comparison with previous work – see text.

References

[1] G. Herzberg, Molecular Spectra and Molecular Structure III: Electronic Spectra and Electronic Structure of Polyatomic Molecules (Krieger, Malabar, 1991).

[2] D. H. Whiffen, J. Chem. Soc., 1350 (1956)

[3] J. E. Purvis, J. Chem. Soc., **99**, 911 (1911)

[4] H. Sponer and S. H. Wollman, J. Chem. Phys., **9**, 816 (1941)

[5] T. Cvitaš and J. M. Hollas, Molec. Phys., **18**, 101 (1970)

[6] H. D. Bist, V. N. Sarin, A. Ojha, and Y. S. Jain, Applied Spec., **24**, 292 (1970)

[7] H. D. Bist, V. N. Sarin, A. Ojha, and Y. S. Jain, Spectrochim. Acta A, **26**, 841 (1970)

[8] Y. S. Jain and H. D. Bist, J. Mol. Spec., **47**,126 (1973)

[9] A. M. Gardner and T. G. Wright. J. Chem. Phys. **135**, 114305 (2011).

[10] J.-I. Murakami, K. Kaya, and M. Ito, J. Chem. Phys., **72**, 3263 (1980)

[11] S. L. Anderson, D. M. Rider, and R. N. Zare, Chem. Phys. Lett., **93**, 11 (1982)

[12] K. Walter, K. Scherm, and U. Boesl, J. Phys. Chem., **95**, 1188 (1991)

[13] A. de la Cruz, J. Campos, and M. Ortiz, J. Mol. Spec., **180**, 305 (1996)

[14] P. Imhof and K. Kleinermanns, Chem. Phys., **270**, 227 (2001)

[15] A. M. Bass and H. Sponer, J. Opt. Soc. **40**, 389 (1950).

[16] H. Schüler and A. Woeldike, Phys. Zeits. **42**, 390 (1941).

[17] A. Woeldike, Zeits. Naturforsch. **1**, 566 (1946).

[18] H. Schüler, Zeits. Naturforsch. A **2**, 556 (1947)

[19] T. R. Nanney, R. T. Bailey, and E. R. Lippincott, Spectrochim. Acta **21**, 1495 (1965).

[20] G. Varsányi, *Assignments of the Vibrational Spectra of Seven Hundred Benzene Derivatives* (Wiley, New York, 1974)

[21] P. Asselin, A. Gouzerh, F. Piuzzi, and I. Dimicoli, Chem. Phys., **175**, 387 (1993)

[22] A. W. Potts, M. L. Lyus, E. P. F. Lee, and G. H. Fattahallah, J. Chem. Soc., Farad. Trans. 2, **76**, 556 (1980).

[23] X. Ripoche, I. Dimicoli, J. Le Calvé, F. Piuzzi, and R. Botter, Chem. Phys. **124**, 305 (1988).

[24] T. G. Wright, S. I. Panov, and T. A. Miller, J. Chem. Phys., **102**, 4793 (1995)

[25] C. J. Kwon, H. L. Kim, and M. S. Kim, J. Chem. Phys. **116**, 10361 (2002).

[26] G. Lembach and B. Brutschy, Chem. Phys. Lett., **273**, 421 (1997)

[27] E. B. Wilson, Jr, Phys. Rev., **45**, 706 (1934)

[28] P. Butler, D. B. Moss, H. Yin, T. W. Schmidt, and S. H. Kable, J. Chem. Phys. **127**, 094303 (2007).

[29] I. Pugliesi, N. M. Tonge, and M. C. R. Cockett, J. Chem. Phys., **129**, 104303 (2008)

[30] J. P. Harris, A. Andrejeva, W. D. Tuttle, I. Pugliesi, C. Schriever, and T. G. Wright, J. Chem. Phys., **141**, 244315 (2014)

[31] R. S. Mulliken, J. Chem. Phys., **23**, 1997 (1955)

[32] G. Herzberg, Molecular Spectra and Molecular Structure II: Infrared and Raman Spectra of Polyatomic molecules (Krieger, Malabar, 1991) p. 272

[33] A. M. Gardner, A. M. Green, V. M. Tame-Reyes, V. H. Wilton, and T. G. Wright, **138**, 134303 (2013)

[34] A. M. Gardner, A. M. Green, V. M. Tame-Reyes, K. L. Reid, J. A. Davis, V. H. K. Parkes, and T. G. Wright, J. Chem. Phys., **140**, 114308 (2014)

[35] F. Duschinsky, Acta Physicochim. URSS **7**, 551 (1937).

[36] *Gaussian 09*, Revision C.01, M. J. Frisch, G. W. Trucks, H. B. Schlegel, G. E. Scuseria, M. A. Robb, J. R. Cheeseman, G. Scalmani, V. Barone, B. Mennucci, G. A. Petersson, H. Nakatsuji, M. Caricato, X. Li, H. P. Hratchian, A. F. Izmaylov, J. Bloino, G. Zheng, J. L. Sonnenberg, M. Hada, M. Ehara, K. Toyota, R. Fukuda, J. Hasegawa, M. Ishida, T. Nakajima, Y. Honda, O. Kitao, H. Nakai, T. Vreven, J. A. Montgomery, Jr., J. E. Peralta, F. Ogliaro, M. Bearpark, J. J. Heyd, E. Brothers, K. N. Kudin, V. N. Staroverov, R. Kobayashi, J. Normand, K. Raghavachari, A. Rendell, J. C. Burant, S. S. Iyengar, J. Tomasi, M. Cossi, N. Rega, J. M. Millam, M. Klene, J. E. Knox, J. B. Cross, V. Bakken, C. Adamo, J. Jaramillo, R. Gomperts, R. E. Stratmann, O. Yazyev, A. J. Austin, R. Cammi, C. Pomelli, J. W. Ochterski, R. L. Martin, K. Morokuma, V. G. Zakrzewski,
G. A. Voth, P. Salvador, J. J. Dannenberg, S. Dapprich, A. D. Daniels, Ö. Farkas, J. B. Foresman, J. V. Ortiz, J. Cioslowski, and D. J. Fox, Gaussian, Inc., Wallingford CT, 2009.

[37] I. Pugliesi and K. Muller-Dethlefs, J. Phys. Chem. A, **110**, 4657 (2006), a free download of the software can be found at http://www.fclab2.net

[38] PGOPHER, a Program for Simulating Rotational, Vibrational and Electronic Structure, C. M. Western, University of Bristol, http://pgopher.chm.bris.ac.uk.

[39] "See supplemental material at [URL will be inserted by AIP] for tables of assignments of the ^{37}ClBz-h_5 and ^{37}ClBz-d_5 spectra, as well as the derived fundamental wavenumbers."

[40] U. Boesl, R. Zimmermann, C. Weickhardt, D. Lenoir, K.-W. Schramm, A. Kettrup, and E. W Schlag, Chemosphere, **29**, 1429 (1994).

[41] R. Vasudev and J. C. D. Brand, J. Molec. Spec. **75**, 288 (1979).

[42] See, for example, Y.-J. Liu, P. Persson, and S. Lunell, J. Phys. Chem. A **108**, 2339 (2004).

[43] T. Deguchi, N. Takeyasu, and T. Imasaka, Appl. Spectrosc. **56**, 1241 (2002).

[44] Y.-Z. Liu, C.-C. Qin, S. Zhang, Y.-M. Wang, and B. Zhang, Acta Phys. -Chim. Sin. **27**, 965 (2011).

[45] T. G. Dietz, M. A. Duncan, M. G. Liverman, and R. E. Smalley, J. Chem. Phys. **73**, 4816 (1980).

[46] J. R. Gascooke, U. N. Alexander, and W. D. Lawrance, J. Chem. Phys. **134**, 184301 (2011).